NAT'L INST. OF STAND & TECH R.I.C.

A11104 882755

NIST PUBLICATIONS

NISTIR 5774

Electronics and Electrical Engineering Laboratory

J. M. Rohrbaugh
Compiler

Technical Progress Bulletin

95-3

Covering Laboratory Programs,
July to September 1995
with 1996 EEEL Events Calendar

U.S. DEPARTMENT OF COMMERCE
Technology Administration
National Institute of Standards and Technology

NIST

QC
100
.U56
NO.5774
1996

NISTIR 5774

Electronics and Electrical Engineering Laboratory

Technical Progress Bulletin

Covering Laboratory Programs,
July to September 1995
with 1996 EEEL Events Calendar

J. M. Rohrbaugh
Compiler

Electronics and Electrical
Engineering Laboratory
Semiconductor Electronics Division
Gaithersburg, MD 20899

January 1996

95-3

U.S. DEPARTMENT OF COMMERCE
Ronald H. Brown, Secretary
TECHNOLOGY ADMINISTRATION
Mary L. Good, Under Secretary for Technology
NATIONAL INSTITUTE OF STANDARDS AND TECHNOLOGY
Arati Prabhakar, Director

ELECTRONICS AND ELECTRICAL ENGINEERING LABORATORY TECHNICAL PROGRESS BULLETIN, JANUARY 1996 ISSUE

INTRODUCTION

This is the fifty-second issue of a quarterly publication providing information on the technical work of the National Institute of Standards and Technology Electronics and Electrical Engineering Laboratory (EEEL). This issue of the EEEL Technical Progress Bulletin covers the third quarter of calendar year 1995.

Organization of Bulletin: This issue contains abstracts for all relevant papers released for publication by NIST in the quarter and citations and abstracts for such papers published in the quarter. Entries are arranged by technical topic as identified in the Table of Contents and alphabetically by first author under each subheading within each topic. Unpublished papers appear under the subheading "Released for Publication." This does not imply acceptance by any outside organization. Papers published in the quarter appear under the subheading "Recently Published." Following each abstract is the name and telephone number of the individual to contact for more information on the topic (usually the first author). This issue also includes a calendar of Laboratory conferences and workshops planned for calendar year 1996 and a list of sponsors of the work.

Electronics and Electrical Engineering Laboratory: EEEL programs provide national reference standards, measurement methods, supporting theory and data, and traceability to national standards. The metrological products of these programs aid economic growth by promoting equity and efficiency in the marketplace, by removing metrological barriers to improved productivity and innovation, by increasing U.S. competitiveness in international markets through facilitation of compliance with international agreements, and by providing technical bases for the development of voluntary standards for domestic and international trade. These metrological products also aid in the development of rational regulatory policy and promote efficient functioning of technical programs of the Government.

The work of the Laboratory is conducted by five technical research Divisions: the Semiconductor Electronics and the Electricity Divisions in Gaithersburg, Md., and the Electromagnetic Fields and the Electromagnetic Technology Divisions, and the newly formed Optoelectronics Division in Boulder, Colo. The Office of Law Enforcement Standards conducts research and provides technical services to the U.S. Department of Justice and State and local governments, and other agencies in support of law enforcement activities. In addition, the Office of Microelectronics Programs (OMP) coordinates the growing number of semiconductor-related research activities at NIST. Reports of work funded through the OMP are included under the heading "Semiconductor Microelectronics."

Key contacts in the Laboratory are listed at the end of this publication; readers are encouraged to contact any of these individuals for further information. To request a subscription or for more information on the Bulletin, write to EEEL Technical Progress Bulletin, National Institute of Standards and Technology, Metrology Building, Room B-358, Gaithersburg, MD 20899 or call (301) 975-2220.

Laboratory Sponsors: The Laboratory Programs are sponsored by the National Institute of Standards and Technology and a number of other organizations, in both the Federal and private sectors; these are identified on page 31.

Note on Publication Lists: Publication lists covering the work of each division are guides to earlier as well as recent work. These lists are revised and reissued on an approximately annual basis and are available from the originating division. The current set is identified in the Additional Information section, page 28.

Certain commercial equipment, instruments, or materials are identified in this paper in order to specify adequately the experimental procedures. Such identification does not imply recommendation or endorsement by the National Institute of Standards and Technology, nor does it imply that the materials or equipment identified are necessarily the best available for the purpose.

TABLE OF CONTENTS

INTRODUCTION . . . ii

FUNDAMENTAL ELECTRICAL MEASUREMENTS . . . 3

SEMICONDUCTOR MICROELECTRONICS . . . 3
- Silicon Materials [includes SIMOX and SOI] . . . 3
- Compound Materials . . . 4
- Analysis and Characterization Techniques . . . 5
- Device Physics and Modeling . . . 6
- Dimensional Metrology . . . 6
- Integrated-Circuit Test Structures . . . 6
- Microfabrication Technology [includes MBE, micromachining, MEMs] . . . 7
- Plasma Processing . . . 7
- Power Devices . . . 8
- Reliability [includes electromigration] . . . 9

SIGNAL ACQUISITION, PROCESSING, AND TRANSMISSION . . . 9
- DC and Low-Frequency Metrology . . . 9
- Cryoelectronic Metrology . . . 9
- Antenna Metrology [includes radar cross section measurements] . . . 13
- Noise Metrology . . . 15
- Microwave and Millimeter-Wave Metrology . . . 15
- Electromagnetic Properties . . . 16
- Laser Metrology . . . 17
- Optical Fiber Metrology . . . 17
- Optical Fiber/Waveguide Sensors . . . 18
- Integrated Optics [includes waveguide structures] . . . 19
- Other Signal Topics . . . 20

ELECTRICAL SYSTEMS . . . 21
- Power Systems Metrology . . . 21
- Magnetic Materials and Measurements . . . 22
- Superconductors . . . 23
- Other Electrical Systems Topics . . . 27

ELECTROMAGNETIC INTERFERENCE . . . 27
- Conducted EMI . . . 27
- Radiated EMI . . . 28

ADDITIONAL INFORMATION . . . 28
- Announcements . . . 28
- List of Publications . . . 29
- 1996 Calendar of Events . . . 29
- EEEL Sponsors . . . 31

TO LEARN MORE ABOUT THE LABORATORY....

Two general documents are available that may be of interest. These are ***Measurements for Competitiveness in Electronics*** and ***EEEL 1994 Technical Accomplishments, Supporting Technology for U.S. Competitiveness in Electronics.*** The first identifies measurement needs for a number of technical areas and the general importance of measurements to competitiveness issues. The findings of each chapter dealing with an individual industry have been reviewed by members of that industry. The second presents selected technical accomplishments of the Laboratory for the period October 1, 1993 through September 30, 1994. A brief indication of the nature of the technical achievement and the rationale for its undertaking are given for each example. A longer description of both documents follows:

Measurements for Competitiveness in Electronics, NISTIR 4583 (April 1993).

Measurements for Competitiveness in Electronics identifies for selected technical areas the measurement needs that are most critical to U.S. competitiveness, that would have the highest economic impact if met, and that are the most difficult for the broad range of individual companies to address. The document has two primary purposes: (1) to show the close relationship between U.S. measurement infrastructure and U.S. competitiveness and show why improved measurement capability offers such high economic leverage, and (2) to provide a statement of the principal measurement needs affecting U.S. competitiveness for given technical areas, as the basis for a possible plan to meet those needs, should a decision be made to pursue this course.

The first three chapters, introductory in nature, cover the areas of: the role of measurements in competitiveness, NIST's role in measurements, and an overview of U.S. electronics and electrical-equipment industries. The remaining nine chapters address individual fields of electronic technology: semiconductors, magnetics, superconductors, microwaves, lasers, optical-fiber communications, optical-fiber sensors, video, and electromagnetic compatibility. Each of these nine chapters contains four basic types of information: technology review, world markets and U.S. competitiveness, goals of U.S. industry for competitiveness, and measurement needs. Three appendices provide definitions of the U.S. electronics and electrical-equipment industries.

This document is a successor to NISTIR 90-4260, *Emerging Technologies in Electronics ... and their measurement needs* [Second Edition].
[Contact: Ronald M. Powell, (301) 975-2220]

EEEL 1994 Technical Accomplishments, Supporting Technology for U.S. Competitiveness in Electronics, NISTIR 5551 (December 1994).

The Electronics and Electrical Engineering Laboratory, working in concert with other NIST Laboratories, is providing measurement and other generic technology critical to the competitiveness of the U.S. electronics industry and the U.S. electricity-equipment industry. This report summarizes selected technical accomplishments and describes activities conducted by the Laboratory in FY 1994 in the field of semiconductors, magnetics, superconductors, low-frequency microwaves, lasers, optical fiber communications and sensors, video, power, electromagnetic compatibility, electronic data exchange, and national electrical standards. Also included is a profile of EEEL's organization, its customers, and the Laboratory's long-term goals.

EEEL is comprised of five technical divisions, Electricity and Semiconductor Electronics in Gaithersburg, Maryland, and Electromagnetic Fields, Electromagnetic Technology, and Optoelectronics in Boulder, Colorado. Through two offices, the Laboratory manages NIST-wide programs in microelectronics and law enforcement.
[Contact: JoAnne Surette, (301) 975-5267]

Internet Access (World Wide Web): http://www.eeel.nist.gov

FUNDAMENTAL ELECTRICAL MEASUREMENTS

Released for Publication

Jeffrey, A., Elmquist, R.E., and Cage, M.E., **Precision Tests of a Quantum Hall Effect Device dc Equivalent Circuit Using Double-Series and Triple-Series**, to be published in the Journal of Research of the National Institute of Standards and Technology.

Precision tests verify the dc equivalent circuit used by Ricketts and Kemeny to describe a quantum Hall effect device in terms of electrical circuit elements. The tests employ the use of cryogenic current comparators and the double-series and triple-series connection techniques of Delahaye. Verification of the dc equivalent circuit in double-series and triple-series connections is a necessary step in developing the ac quantum Hall effect as an intrinsic standard of resistance.
[Contact: Randolph E. Elmquist, (301) 975-6591]

FUNDAMENTAL ELECTRICAL MEASUREMENTS

Recently Published

Lee, K.C., **The Quantum Hall Effect-Based Resistance Standard: Capabilities and Implementation**, Proceedings of the Eighteenth Annual Workshop of NASA Metrology and Calibration 1995, Greenbelt, Maryland, April 18-20, 1995, Section 6, pp. 1-6.

In order to support modern 8 1/2-digit digital multimeters and high-accuracy calibrators capable of delivering uncertainties of the order of parts per million (ppm), primary standards laboratories must be able to provide calibration uncertainties less than 0.1 ppm. Quantum Hall effect-based resistance standards can provide these low uncertainties, but at present require very sophisticated and costly equipment. This talk describes the quantum Hall effect (QHE), the equipment necessary to use it as a resistance standard, and some of the challenges in making a QHE-based resistance standard commercially viable.
[Contact: Kevin C. Lee, (301) 975-4236]

SEMICONDUCTOR MICROELECTRONICS

Silicon Materials

Recently Published

Jacobs, C., Genis, A., Allen, L.P., and Roitman, P., **Effect of Anneal Temperature on Si/Buried Oxide Interface Roughness of SIMOX**, Proceedings of the 1994 IEEE SOI Conference, Nantucket, Massachusetts, October 3-6, 1994, pp. 49-50.

Fully depleted, thin-film silicon-on-insulator (SOI) SIMOX devices are attractive for their short-channel characteristics and high speed compared with bulk silicon. Their potential for applications in low power devices and circuitry places extreme demands upon the starting SIMOX substrate material. Threshold voltage control for fully depleted SOI devices has been recognized as a key issue for realization of fully depleted SOI technology. To that end, examination of the interface roughness between the device silicon layer and the buried oxide of the SOI structure is an active area of materials research and development. In this work, we have used atomic force microscopy to measure the interface roughness of SIMOX SOI substrates as a function of anneal parameters. This study has shown that the silicon/buried oxide interface roughness is a strong function of the post-implant annealing temperature.
[Contact: Peter Roitman, (301) 975-2077]

Kopanski, J.J., **Oxidation of SiC**, in Properties of Silicon Carbide, Chapter 5.2, G. L. Harris, Ed. (INSPEC, the Institution of Electrical Engineers, London, United Kingdom, 1995), pp. 121-129.

Thermal oxidation of the two most common forms of single-crystal silicon carbide with potential for semiconductor electronics applications is discussed: 3C-SiC formed by heteroepitaxial growth by chemical vapor deposition on silicon, and 6H-SiC wafers grown in bulk by vacuum sublimation or the Lely method. SiC is also an important ceramic and abrasive that exists in many different forms. Its oxidation has been studied under a wide variety of conditions. Thermal oxidation of SiC for semiconductor electronic applications is discussed. Insulating layers on SiC, other than thermal oxide, and the electrical properties of the thermal oxide and metal-oxide-semiconductor capacitors formed on SiC are also discussed.
[Contact: Joseph J. Kopanski, (301) 975-2089]

Lee, J.D., Park, J.C., Krause, S., and Roitman, P., **Defect Formation Mechanism Causing Increasing Defect Density During Decreasing Implant Dose in Low-Dose SIMOX**, Proceedings of the 1994 IEEE SOI Conference, Nantucket, Massachusetts, October 3-6, 1994, pp. 69-70.

Silicon-on-insulator material synthesized by oxygen implantation (SIMOX) is a leading candidate for advanced large-scale integrated-circuit applications due to thickness uniformity and moderate defect density. In the past few years, there has been a significant reduction of the defect density by optimizing processing conditions. Today, commercial SIMOX wafers are available by single implant at a high dose of 1.8×10^{18} cm^{-2} (defect density $\sim 10^6$ cm^{-2}), single implant at a low dose of $\sim 0.5 \times 10^{18}$ cm^{-2} (defect density $<10^3$ cm^{-2}), and multiple implants/anneals (defect density $<10^4$ cm^{-2}). Studies on defect formation mechanisms may suggest further modification of the processing conditions for both production cost and material quality. Recently, it was shown that through-thickness defects in high-dose SIMOX originated from as-implanted defects, dislocation half-loops. On the other hand, a high density ($\sim 10^8$ cm^{-2}) of defects has not been understood. In this paper, we report on the effect of implant dose on defect formation mechanisms, and propose a defect formation mechanism in very low-dose regime for the first time.
[Contact: Peter Roitman, (301) 975-2077]

Sadana, D.K., Lasky, J., Hovel, H.J., Petrillo, K., and Roitman, P., **Nano-Defects in Commercial Bonded SOI and SIMOX**, Proceedings of the 1994 IEEE SOI Conference, Nantucket, Massachusetts, October 3-6, 1994, pp. 111-112.

Two new classes of defects have been identified in commercial Separation by IMplantation of OXygen (SIMOX), plasma thinned bonded silicon-on-insulator (BSOI) and bonded etched silicon-on-insulator (BESOI) materials. The first class of defects is revealed when the materials are treated in concentrated HF, and their density is in the range 10^2 to 10^3 cm^{-2}. The second class of defects appears when the materials are etched by the enhanced Secco etch method. Contrary to the common belief, defect densities of 10^4 to 10^5 cm^{-2} are present in both plasma-thinned BSOI and BESOI after Secco etching. The defect densities in SIMOX after the Secco etching were 10^6 to 10^7 cm^{-2}, which was expected.
[Contact: Peter Roitman, (301) 975-2077]

Twigg, M.E., Hughes, H.L., Roitman, P., and Allen, L.P., **Measurement of Low Defect Densities in SIMOX Using Transmission Electron Microscopy**, Proceedings of the 1994 IEEE SOI Conference, Nantucket, Massachusetts, October 3-6, 1994, pp. 85-86.

In order to reduce short-channel effects for devices with channel lengths less than 0.25 μm, the buried oxide (BOX) thickness will need to be less than 200 nm. To this end, an experimental low-dose ($0.7 \times 10^{18}/cm^2$) oxygen implantation process for thin-BOX SIMOX has been explored. The extended defects in this material are predominantly dislocation pairs that run from the superficial Si/BOX interface to oxide precipitates. As in all electronic materials, the dislocation density in the device region must also be minimized. A reduction in the superficial Si layer dislocation density from $\sim 10^7/cm^2$ to an estimated value of less than $100/cm^2$ was achieved by subjecting this material to prolonged (16-h) anneal at 1325 °C in an atmosphere of 0.5% O_2 in Ar. The anneal effectively reduced the device silicon layer from 270 nm to 200 nm as measured by cross-sectional TEM. The BOX layer thickness was unchanged by the anneal and remained at 130 nm.
[Contact: Peter Roitman, (301) 975-2077]

Compound Materials

Released for Publication

Kim, J.S., Lowney, J.R., and Thurber, W.R., **Transport Properties of Narrow-Gap II-VI Compound Semiconductors**.

The present understanding of the transport properties and their specific measurement methodologies in narrow-gap semiconductors, mainly the HgCdTe ternary system, are overviewed. Because of the importance of the multicarrier approach to the electrical characterization of advanced semiconductor materials, structures, or devices, the reduced-conductivity-tensor (RCT) scheme of multicarrier analysis is discussed in detail. Selected RCT data and their implications are also presented. The two-

terminal magnetoresistance and high-magnetic-field measurement methods are also discussed.
[Contact: Jin S. Kim, (301) 975-2238]

Compound Materials

Recently Published

Bennett, H.S., **Summary Report of the Workshop on Planning for Compound Semiconductor Technology**, NISTIR 5702 (August 1995).

This report describes the motivation for and the results of the Workshop on Planning for Compound Semiconductor Technology. It also includes copies of the viewgraphs used by the speakers at the Workshop. This Workshop, sponsored by the National Institute of Standards and Technology and the Semiconductor Equipment and Materials International, was held at Gaithersburg, Maryland on February 3, 1995.

The purposes of the Workshop were to assess whether agreement exists in the compound semiconductor industry on the need for a consensus-based planning effort and to foster the free exchange of information and ideas that might be used to create a more competitive compound semiconductor industry.

The Workshop attendees agreed that a consensus on the need for such planning does exist, and that if such planning occurs, it is more appropriate to use existing industry and government organizations. The attendees also proposed the four future actions of 1) forming an industrial alliance on planning for compound semiconductors; 2) coordinating the activities of the proposed compound semiconductor alliance with related activities in government agencies; 3) determining to what extent the government agencies and other interested parties are able to provide funds and/or staff to form the compound semiconductor alliance; and 4) forming a parallel organization for the microwave/radio frequency industry that addresses questions similar to those addressed by Optoelectronics Industry Development Association for optoelectronics.
[Contact: Herbert S. Bennett, (301) 975-2079]

Kim, J.S., Seiler, D.G., Colombo, L., and Chen, M.C., **Characterization of Liquid-Phase Epitaxially Grown HgCdTe Films by Magnetoresistance Measurements**, Journal of Electronic Materials, Vol. 24, No. 9, pp. 1305-1310 (1995).

In this paper, we demonstrate that measurements of the magnetoresistance can be used as a valuable alternative to conventional characterization tools to study transport properties of advanced semiconducting materials, structures, or devices. We have measured magnetoresistance on two different systems, namely, three liquid-phase epitaxially grown HgCdTe films and two GaAs-based high-electron-mobility-transistor (HEMT) structures. The results are analyzed by using a two-carrier model as a reference in the context of the reduced-conductivity-tensor scheme. The HEMT data are in quantitative agreement with the two-carrier model, but the HgCdTe data exhibit appreciable deviations from the model. The observed deviations strongly indicate a mobility spread and material complexity in the HgCdTe samples which are probably associated with inhomogeneities and the resulting anomalous electrical behavior.
[Contact: Jin S. Kim, (303) 975-2238]

Analysis and Characterization Techniques

Recently Published

Dagata, J.A., and Kopanski, J.J., **Scanning Probe Techniques for the Electrical Characterization of Semiconductor Devices**, Solid State Technology, pp. 91-97 (July 1995).

The spatial resolution, sensitivity, and accuracy required for electrical characterization of device structures in the semiconductor industry suggest that scanning probe microscopy (SPM) tools may offer an alternative to existing measurement techniques. Due to their two-dimensional imaging capabilities, high-spatial resolution, and nondestructive nature, SPM-based characterization tools are evolving from lab to fab. This article examines the current standard of performance for electrical measurements of semiconductor devices and the prospects for the application of SPM as a next-generation tool for dopant profiling and defect inspection of device structures.
[Contact: Joseph J. Kopanski, (301) 975-2089]

Schaafsma, D.T., and Christensen, D.H., **Cross-**

Sectional Photoluminescence and Its Application to Buried-Layer Semiconductor Structures, Journal of Applied Physics, Vol. 78, No. 2, pp. 694-699 (July 15, 1995).

We present an overview of a cross-sectional scanning microphotoluminescence technique. This technique is used to examine various buried-layer semiconductor structures for which traditional surface-normal techniques cannot yield sufficient information or must be coupled with time-consuming and painstaking processes such as wet etching. This technique has a wide range of applications; two applications, defect-driven interdiffusion in quantum wells and the modification of spontaneous emission from quantum wells in vertical-cavity surface-emitting lasers (VCSELs), are discussed here. The data obtained using this method can be used to distinguish emission spectra from quantum wells as little as 1 μm apart in depth and a few nanometers different in wavelength. The comparison of normal-incidence with cross-sectional data from VCSELs can be used to more effectively optimize the match between cavity resonance and quantum-well emission in high-Q devices. The physical model for an oscillating dipole in a planar cavity leads to an interesting conclusion about the dependence of the emission spectrum on the location of the dipole, namely, that an emitter inside a Fabry-Perot cavity will have the same spectrum as an identical one located a corresponding distance outside of the cavity. This conclusion is tested experimentally, using a VCSEL structure with emitters distributed inside and outside the effective cavity length.
[Contact: David H. Christensen, (303) 497-3354]

Device Physics and Modeling

Recently Published

Lowney, J.R., **Model for Determining the Density and Mobility of Carriers in Thin Semiconducting Layers with Only Two Contacts**, Journal of Applied Physics, Vol. 78, No. 2, pp. 1008-1012 (15 July 1995).

A new method for determining the carrier densities and mobilities in a thin semiconducting layer was recently described. It is based on fitting the transverse magnetoresistance of the layers as a function of magnetic field, and it requires only two contacts. To improve the accuracy and generalize the procedure to multicarrier systems, a computer code was written to solve for the magnetoresistance as a function of magnetic field and the length-to-width ratio of a rectangular sample. A nonlinear least-squares fit was made to the results of the computer model for a single-carrier system. The results for multi-carrier systems are discussed. This method is especially useful as a monitor for improving the quality control of the electrical characteristics of thin conducting layers in finished devices. The code is also useful for interpreting standard four-terminal measurements as well.
[Contact: Jeremiah R. Lowney, (301) 975-2048]

Dimensional Metrology

Recently Published

Lowney, J.R., **MONSEL-II Monte Carlo Simulation of SEM Signals for Linewidth Metrology**, Microbeam Analysis, Vol. 4, pp. 131-136 (1995).

This is a guide to the FORTRAN code MONSEL-II, which is a Monte Carlo simulation of the transmitted, backscattered, and secondary electron signals in a scanning electron microscope (SEM) associated with lines with a trapezoidal cross section. The lines are deposited on a multilayer substrate. The primary purpose of the code is to interpret the actual linewidths from measured SEM signals. However, it can be used for many other purposes such as transmission electron microscopy.
[Contact: Jeremiah R. Lowney, (301) 975-2048]

Integrated-Circuit Test Structures

Recently Published

Schuster, C.E., ***Semiconductor Measurement Technology*: Test Structure Implementation Document: DC Parametric Test Structures and Test Methods for Monolithic Microwave Integrated Circuits (MMICs)**, NIST Special Publication 400-97 (September 1995).

This document describes a set of microelectronic test structure designs for manufacturers of GaAs MMIC devices. These designs enable the dc measurement of process and device parameters

that can be used to diagnose, monitor, compare, and predict the performance of the fabrication process or the devices produced. The test structure designs are embodied in a computer-aided design library known at NISTGAAS, which contains eight types of test structures, implemented in 125 combinations of process layer and size, and based on a 2 x 6 probe-pad array. Any design, once fabricated on a wafer, can be probed using commonly available commercial parametric test system equipment. This document specifies how to implement and test each type of test structure and how to analyze the results. It also provides guidance on how to apply the set of test structures at the wafer level. Although NISTGAAS was designed for the process described in this document, it was also designed and demonstrated to be adaptable for other MMIC processes. Since NISTGAAS contains cell designs rather than a chip design, it provides a flexible test structure methodology that also provides the MMIC community with a common reference point for assessing process and device performance.
[Contact: Constance E. Schuster, (301) 975-2241]

Microfabrication Technology

Recently Published

Gaitan, M., **MEMS in Standard CMOS VLSI Technology**, Proceedings of the Twenty-Ninth Annual Conference on Information Sciences and Systems, Baltimore, Maryland, March 22-24, 1995, pp. 169-173.

The methodology for the design and fabrication of a class of thermo-electro-mechanical devices and systems that can be fabricated in a commercial CMOS foundry environment is presented. The fabrication technique allows the monolithic integration of the micromechanical devices with CMOS VLSI circuits using standard design methods. Microheating elements and thermoelectric sensors are presented as examples of the application of this technique.
[Contact: Michael Gaitan, (301) 975-2070]

Plasma Processing

Recently Published

Olthoff, J.K., Van Brunt, R.J., and Radovanov, S.B., **Effect of Electrode Material on Measured Ion Energy Distributions in Radio-Frequency Discharges**, Applied Physics Letters, Vol. 67, No. 4, pp. 473-475 (July 24, 1995).

The influence of electrode surface material and conditions on the measurement of kinetic-energy distributions of ions sampled through an orifice in the grounded electrode of a parallel-plate, capacitively-coupled radio-frequency discharge cell has been investigated for discharges generated in different gas mixtures. Significant shifts in energy and/or discrimination of low-energy ions are observed for aluminum electrodes or for stainless-steel electrodes on which aluminum appears to have been deposited by sputtering. Their effects are considerably reduced in the case of stainless-steel electrodes that have been freshly cleaned and polished. It is argued that the observed energy shifts are attributable to charging of oxide layers on the electrode surface around the sampling orifice.
[Contact: James K. Olthoff, (301) 975-2431]

Radovonov, S.B., Olthoff, J.K., Van Brunt, R.J., and Djurovic, S., **Ion Kinetic-Energy Distributions and Balmar-alpha (H_α) Excitation in Ar-H_2 Radio-Frequency Discharges**, Journal of Applied Physics, Vol. 78, No. 2, pp. 746-757 (July 15, 1995).

Excited neutrals and fast ions produced in a 13.56 MHz radio-frequency discharge in a 90% argon - 10% hydrogen gas mixture were investigated, respectively, by spatially and temporally resolved optical emission spectroscopy, and by mass-resolved measurements of ion kinetic energy distributions at the grounded electrode. The electrical characteristics of the discharge were also measured, and comparisons are made with results obtained for discharges in pure H_2 under comparable conditions. Measurements of Balmer-alpha (H_α) emission show Doppler-broadened emission that is due to the excitation of fast atomic hydrogen neutrals formed with ion neutralization processes in the discharge. Temporally and spatially resolved emission profiles of the H_α radiation from the Ar-H_2 mixture are presented for the "slow" component produced predominately by electron-impact dissociative excitation of H_2, and for the "fast" component corresponding to energies much greater

than can be derived from dissociative excitation. For the Ar-H_2 mixture, the fast component is significantly enhanced relative to the slow component. The measured, kinetic-energy distributions and fluxes of predominant ions in the Ar-H_2 mixture, such as H_3^+, H_2^+, H^+, and ArH^+, suggest mechanisms for the formation of fast hydrogen atoms. The interpretation of results indicate that H^+ and/or H_3^+, neutralized and backscattered by collision with the powered electrode, are the likely sources of fast hydrogen atoms that produce Doppler-shifted H_α emission in the discharge. There is also evidence at the highest pressures and voltages of "runaway" H^+ ions formed near the powered electrode, and detected with kinetics energies exceeding 100 eV at the grounded electrode.
[Contact: Svetlana B. Radovanov, (301) 975-2436]

Rao, M.V.V.S., Radovanov, S.B., Van Brunt, R.J., and Olthoff, J.K., **Kinetic Energy Distribution of Ions Produced from Townsend Discharges in Neon and Argon**, Proceedings of the Nineteenth International Conference on Physics of Electronic and Atomic Collisions, Whistler, British Columbia, Canada, July 26—August 1, 1995, p. 392.

Study of the kinetic energy distribution (KED) of various ions produced in the breakdown of a gas under the influence of a uniform dc electric field at various electric field to gas density (E/N) ratios provides important information on the relative role of elastic and inelastic collision processes which occur in transporting ions within the discharge sheath region. In this paper, we present our results on the measurements of KEDs of Ne^+ in Ne and Ar^+ in a low-current diffuse Townsend discharges. The discharges are generated between two plane and circular parallel plates. The discharge cell is coupled to a cylindrical mirror analyzer (CMA) in conjunction with a quadrupole mass spectrometer (QMS). The ions sampled through a 0.1 mm orifice at the center of the discharge are energy analyzed by the CMA, and subsequently, separated according to their mass to charge ratio (m/z) by the QMS. More details on the apparatus and data acquisition system have been discussed elsewhere.
[Contact: Richard J. Van Brunt, (301) 975-2425]

Van Brunt, R.J., Olthoff, J.K., and Radovanov, S.B., **Influence of Electrode Material on Measured Ion Kinetic-Energy Distributions in Radio-Frequency Discharges**, Proceedings of the XXII International Conference on Phenomena in Ionized Gases, Hoboken, New Jersey, July 31—August 4, 1995, pp. 29-30.

The measurement of ion kinetic energies is important for understanding processes that occur in discharges, e.g., the influence of ions on the etching of semiconductor materials in plasma reactors. Direct measurements of ion kinetic energies striking surfaces exposed to the discharge requires sampling through an orifice in a surface. Difficulties with ion sampling through a small aperture, manifested by errors or distortions in measured ion kinetic-energy distributions, have been encountered in previous investigations of both dc and radio-frequency discharges. The errors are usually most significant at relatively low ion energies.
[Contact: Richard J. Van Brunt, (301) 975-2425]

Power Devices

Released for Publication

Adams, V.H., Joshi, Y., and Blackburn, D.L., **Natural Convection from an Array of Electronic Packages Mounted on a Narrow Aspect Ratio Enclosure**, to be published in the Proceedings of the Thirteenth National Heat and Mass Transfer Conference, Surathkal, India, December 28-30, 1995.

Three-dimensional natural convection flow and heat transfer were numerically studied for a 3 x 3 array of discretely heated electronic packages mounted on a horizontal circuit board in an air-filled, narrow aspect ratio rectangular enclosure with length, width, and height ratio of 6:6:1. The governing equations for natural convection in air, coupled with conjugate conduction within the electronic packages and circuit board, were solved using a finite volume method. Nusselt numbers for the package surfaces and maximum chip temperatures for Rayleigh numbers of 10^4, 10^6, and 10^7 were compared with corresponding results from an analysis involving only heat conduction. It was found that conduction-only analysis under-predicts heat transfer from the top surfaces of the electronic packages by a factor of 1.5 to 4.4, with a resultant over-prediction of the maximum chip to ambient temperature difference of 235%.

[Contact: David L. Blackburn, (301) 975-2068]

Reliability

Released for Publication

Schafft, H.A., Erhart, D.L., and Gladden, W.K., **From Testing-In to Building-In Reliability**, to be published in the Proceedings of RELECTRONIC '95 Ninth Symposium on Quality and Reliability in Electronics, Budapest, Hungary, October 16-18, 1995.

Testing-in reliability, as with post-process and life testing, is shown to be no longer a viable response to the aggressive reliability and market-entry demands facing the semiconductor industry. A building-in reliability approach based on identifying and controlling the causes for reduced reliability is described, and examples of its use given.
[Contact: Harry A. Schafft, (301) 975-2234]

Schafft, H.A., Erhart, D.L., and Gladden W.K., **Toward a Building-In Reliability Approach**.

Testing-in reliability, as with post-process and life testing, is shown to be no longer a viable response to the aggressive reliability and market-entry demands facing the semiconductor industry. A building-in reliability approach based on identifying and controlling the causes for reduced reliability is described and compared to the traditional testing-in reliability approach. Specific examples of a building-in reliability approach are given.
[Contact: Harry A. Schafft, (301) 975-2234]

SIGNAL ACQUISITION, PROCESSING, AND TRANSMISSION

DC and Low-Frequency Metrology

Released for Publication

Dulcie, L.L., **A Prototype Apparatus for Determining Changes in the Electrical Conductivity of Production Run Carbon Fibers**, to be published in the Proceedings of the 22nd Annual Quantitative Non-Destructive Evaluation Conference, Seattle, Washington, July 31—August 4, 1995.

A prototype system was developed to detect the small changes in conductivity that occur in carbon fibers when either the heat treatment temperature (HTT) or resident furnace time varies during a production run. This system was designed using an optimized, encircling eddy current coil transducer, appropriate bridge electronics to detect and amplify the signal produced by coil impedance changes, and a voltage output proportional to changes in conductivity along the length of a carbon tow (multiple fibers). System measurement performance was evaluated by comparing the relative changes in output voltage between tows with small variations in conductivities over the HTT range, 1600 °C to 2400 °C. The system successfully tracked single-fiber, absolute conductivities which were measured with a four-wire, dc apparatus developed earlier at NIST.
[Contact: Laura L. Dulcie, (303) 497-5606]

Cryoelectronic Metrology

Released for Publication

Booi, P.A.A., and Benz, S.P., **Detection of 0.85 mW at 240 GHz from Josephson-Junction Arrays**.

We have experimentally coupled emission from a distributed series array to an on-chip 56 Ω load, and detected 0.85 mW at 240 GHz and >100 μW in the range 100 to 300 GHz. The detected power agrees with all 1,968 junctions being phase-locked when we assume a surface resistance of 36 mΩ. This result was achieved using a fabrication process which minimizes the parasitic inductance associated with shunt resistors to 20 fH so that junctions with a 23 mA critical currents could be used.
[Contact: Samuel P. Benz, (303) 497-5258]

Booi, P.A.A., and Benz, S.P., **High-Power, High-Frequency Oscillators Using Distributed Josephson-Junctions Arrays**,

We present experimental results of emission that is coupled from distributed series arrays of wide, resistively-shunted tunnel junctions to on-chip high-ohmic loads. Power levels as high as 0.85 mW near 240 GHz, and power >100 μW at most frequencies in the range 100 to 300 GHz are detected.

[Contact: Samuel P. Benz, (303) 497-5258]

Irwin, K.D., Hilton, G.C., Martinis, J.M., and Cabrera, B., **A Hot Electron Microcalorimeter for X-Ray Detection Using a Superconducting Transition Edge Sensor with Electrothermal Feedback**, to be published in the Proceedings of the 6th International Workshop on Low Temperature Detectors, Interlaken, Switzerland, August 27—September 1, 1995.

We are developing a novel hot electron microcalorimeter for X-ray detection. The absorber consists of a normal metal film which is in thermal and electrical contact with a superconducting transition edge sensor. The superconducting transition-edge sensor is formed by a proximity effect bilayer of aluminum and silver, with a sharp T_c near 100 mK. The temperature of the superconducting film is held constant within its transition by electrothermal feedback, while the substrate temperature is cooled to well below the film temperature. Energy from X-rays absorbed in the normal film is compensated for by a reduction in feedback Joule heating in the superconducting film, which is measured using a series array of dc superconducting quantum interference devices. The feedback mode of operation allows the measurement of incident energy with no free parameters and should lead to improvement in detector resolution over conventional transition edge sensors. In this work, we present an overview of the operation of such a device, describe the aluminum-silver proximity bilayer technology, and present the first results indicating stable detector biasing in the extreme electrothermal feedback regime.
[Contact: John M. Martinis, (303) 497-3597]

Kunkel, G., and Ono, R.H., **Mutual Phase Locking of Ten $Yba_2Cu_3O_{7-x}$ Step-Edge Josephson Junctions up to 45 K**.

We have developed a microwave circuit using ten parallel-biased high-temperature superconductor Josephson junctions to demonstrate phase locking for applications such as oscillators, mixers and detectors. The basic cell consists of two Josephson junctions enclosed in a microstrip resonator which provides in-phase synchronization and low dynamic resistance in the current-voltage characteristic. Synchronization of the ten junctions was observed up to 45 K and up to 1 THz. The theoretical linewidth calculated from the measured dynamic resistance yields values on the order of 2 MHz at 500 GHz and 20 K for the array.
[Contact: Ronald H. Ono, (303) 497-3762]

Martinis, J.M., **Hot Electron Microcalorimeters with 0.25 mm^2 Area**, to be published in the Proceedings of the 6th International Workshop on Low Temperature Detectors, Interlaken, Switzerland, August 27—September 1, 1995.

I present measurements on a hot-electron microcalorimeter with a normal-insulator superconductor tunnel-junction thermometer that is used for the detection of X-rays. With an absorber area of 0.5 mm by 0.5 mm, pulses of 20 μs in duration were observed that gave a 30 eV full width at half maximum resolution for 6 keV X-rays and an 18 eV resolution for heat pulses. This detector has sufficient performance of resolution, detector area, and speed to warrant application in materials analysis.
[Contact: John M. Martinis, (303) 497-3597]

Ono, R.H., Vale, L.R., Reintsema, C.D., and Kunkel, G., **Controlling the Critical Current Density of High Temperature Superconducting Josephson Junctions**, to be published in the Proceedings of the 5th International Superconductive Electronics Conference, Nagoya, Japan, September 18-21, 1995.

High-T_c Josephson junctions have been made using a step-edge superconductor-normal-superconductor process where the critical current density has been controlled by the geometric length of the N region. We discuss techniques for controlling the critical currents while simultaneously adjusting the normal resistances.
[Contact: Ronald H. Ono, (303) 497-3762]

Sanders, S.C., Ekin, J.W., and Jenneret, B., **Pt Buffer Layer for Protecting YBCO from Aluminum at Annealing Temperatures up to 450 °C**.

We have studied the effectiveness of different buffer layers to protect $YBa_2Cu_3O_{7-\delta}$ (YBCO) from aluminum when annealing at temperature up to 450 °C. Since Al is commonly used to form ohmic contacts to Si, these results have implications for

potential hybrid superconductor-semiconductor applications. Buffer layers of Ag, Au, Au/Ag, Au/Cr, Au/Pt, and Pt were examined. The critical temperature (T_c) of the YBCO layer was measured before and after a 300 °C to 450 °C anneal in 1 atm oxygen. Pt and Au/Pt were found to be effective at preventing significant Al diffusion into YBCO and subsequent T_c degradation. The critical current density (J_c) could also be maintained when these buffer layers were employed.
[Contact: Steven C. Sanders, (303) 497-5096]

Cryoelectronic Metrology

Recently Published

Benz, S.P., Reintsema, C.D., and Ono, R.H., **Step-Edge and Stacked-Heterostructure High-T_c Josephson Junctions**, IEEE Transactions on Applied Superconductivity, Vol. 5, No. 2, pp. 2915-2918 (June 1995).

We have explored two high-transition-temperature Josephson junction technologies for application in voltage standard arrays: step-edge junctions made with $YBa_2Cu_3O_{7-\delta}$ and Au normal-metal bridges, and stacked series arrays of Josephson junctions in selectively doped, epitaxially grown $Bi_2Sr_2CaCu_2O_8$ heterostructures. For both kinds of junctions, Shapiro steps induced by a microwave bias were characterized as a function of power. We compare the two technologies with respect to critical current and normal resistance uniformity, maximum achievable critical current, critical-current normal-resistance product, and operating temperature.
[Contact: Samuel P. Benz, (303) 497-5258]

Booi, P.A.A., and Benz, S.P., **Resonances in Two-Dimensional Array Oscillator Circuits**, IEEE Transactions on Applied Superconductivity, Vol. 5, No. 2, pp. 2899-2902 (June 1995).

We present experimental results on the emission from phase-locked two-dimensional arrays of Josephson junctions. We have coupled the emission from 10 x 10 arrays to a room-temperature mixer through a fin-line antenna and WR-12 waveguide. A single voltage-tunable peak was detected up to 230 GHz. A stripline resonance in the antenna reduced the array's dynamic resistance and, thereby, the emission linewidth to as low as 10 kHz. We extract an effective noise temperature of 14 K from the linewidth data. When the array's emission was coupled to an on-chip detector junction through a dc blocking capacitor, we detected voltage-tunable emission from 75 GHz to 300 GHz, and in some circuits, emission above 400 GHz. Here, the coherent power spectrum depends primarily on internal resonances.
[Contact: Peter A. A. Booi, (303) 497-5910]

Doderer, T., Lachenmann, S.G., Huebener, R.P., Booi, P.A.A., and Benz, S.P., **Direct Observation of Vortex Dynamics in Two-Dimensional Josephson-Junction Arrays**, IEEE Transactions on Applied Superconductivity, Vol. 5, No. 2, pp. 2723-2726 (June 1995).

Spatially resolved images of the dynamic states of current-biased overdamped two-dimensional arrays of Nb/AlO_x/Nb Josephson junctions were obtained using low-temperature scanning electron microscopy. We present two-dimensional imaging results describing various vortex dynamic regimes in zero applied magnetic field. The nucleation of current-induced vortices at the array boundaries and their subsequent motion into the array interior are observed for bias currents slightly above the array critical current. With increasing bias current, vortex-vortex interaction becomes important. Discussions on the coherent microwave radiation emission are presented.
[Contact: Peter A. A. Booi, (303) 497-5910]

Eckstein, J.N., Bozovic, I., Virshup, G.F., Ono, R.H., and Benz, S.P., **Stacked Series of High-T_c Trilayer Josephson Junctions**, IEEE Transactions on Applied Superconductivity, Vol. 5, No. 2, pp. 3284-3287 (June 1995).

We report on the properties of stacked series arrays of trilayer Josephson junctions grown by atomic layer-by-layer molecular beam epitaxy. Trilayer Josephson junctions oriented so that the current travels in the c-axis direction have been described previously. Series arrays are made by placing more than one barrier layer in the BSCCO-based epitaxial structure. Single molecular layers of BSCCO-2212 doped with Dy to reduce the local carrier concentration are used as barriers, and are placed very closed to each other, e.g., separated by only a few molecular layers of the superconducting phase.

Phase locking of ac Josephson currents has been observed. The critical current density of such junctions has been observed to be very uniform on wafers that are free of second-phase defects, and operation up to 60 K has been obtained.
[Contact: Ronald H. Ono, (303) 497-3762]

Grossman, E.N., Vale, L.R., Rudman, D.A., Zink, L.R., and Evenson, K.M., **30 THz Mixing Experiments on High Temperature Superconducting Josephson Junctions**, IEEE Transactions on Applied Superconductivity, Vol. 5, No. 2, pp. 3061-3064 (June 1995).

We have investigated $YBa_2Cu_3O_{7-\delta}$ superconductor-normal-superconductor Josephson junctions as mixers of 30 THz radiation. We have directly observed (second-order) difference frequencies from 10 MHz to 12.8 GHz between two CO_2 laser lines. Applying a third microwave signal to the junction, we have observed CO_2 laser difference frequencies up to 27 GHz. The dc bias dependence of the difference frequency signal, as well as other evidence, suggests two distinct mixing mechanisms: hot-electron mixing in the junction banks at high-dc biases, and bolometric Josephson mixing at low-dc biases. The latter is the first observation of Josephson mixing at CO_2 laser frequencies in high-T_c junctions. The Josephson mixing has generated observable mixing products up to sixth order.
[Contact: Erich N. Grossman, (303) 497-5102]

Irwin, K.D., Nam, S.W., Cabrera, B., Chugg, B., Park, S.G., Welty, R.P., and Martinis, J.M., **A Self-Biasing Cryogenic Particle Detector Utilizing Electrothermal Feedback and a SQUID Readout**, IEEE Transactions on Applied Superconductivity, Vol. 5, No. 2, pp. 2690-2693 (June 1995).

We are developing and testing a new type of superconducting transition edge sensor for phonon-mediated particle detection. This sensor consists of a superconducting tungsten thin film deposited on a silicon substrate. The temperature of the film is held constant within the superconducting transitions (T_c = 70 mK) by a feedback process, with the substrate temperature well below the film temperature. Phonon energy deposited in the film is removed by a reduction in feedback Joule heating, which is measured using a series array of dc superconducting quantum interference devices. The resulting signals show improvements in linearity and signal-to-noise ratio over our previous transition edge sensors.
[Contact: John M. Martinis, (303) 497-3597]

Kautz, R.L., **Phase Locking in Two-Dimensional Josephson Junction Arrays: Effect of Critical-Current Nonuniformity**, IEEE Transactions on Applied Superconductivity, Vol. 5, No. 2, pp. 2702-2706 (June 1995).

Numerical simulations are used to study mutual phase locking in two-dimensional arrays of Josephson junctions for parameters typical of successful millimeter-wave oscillators. Such arrays are shown to be very tolerant of random critical-current nonuniformities. However, comparison with an equivalent series array reveals that the locking between rows in a two-dimensional array is principally due to feedback through the external load and not to internal coupling between rows.
[Contact: Richard L. Kautz, (303) 497-3391]

Missert, N.N., Vale, L.R., Ono, R.H., Reintsema, C.D., Rudman, D.A., Thomson, R.E., and Berkowitz, S.J., **Temperature Dependence and Magnetic Field Modulation of Critical Currents in Step-Edge SNS YBCO/Au Junctions**, IEEE Transactions on Applied Superconductivity, Vol. 5, No. 2, pp. 2969-2972 (June 1995).

We compare the electrical transport properties of superconductor-normal metal-superconductor (SNS) step-edge YBCO/Au junctions where the Au is deposited at 100 °C and 600 °C. For both types of junctions, we observe resistively shunted junctions current-voltage characteristics. The critical currents I_c in all cases are similar for a given YBCO thickness to step height ratio, while the normal resistance R_n for the Au deposited at 600 °C is consistently 25% lower. The normalized temperature dependence of the I_cR_n product is identical for all junctions with Au deposited at high temperatures and varies among junctions on a single chop for Au deposited at 100 °C. Low magnetic field modulation of the critical current can show either the expected Fraunhoffer-like pattern or a double-junction modulation for both types of devices. The modulation period is consistently a factor of three lower for the high-temperature deposited Au.

[Contact: Leila L. Vale, (303) 497-5121]

Reintsema, C.D., Ono, R.H., Barnes, G., Borcherdt, L., Harvey, T.E., Kunkel, G., Rudman, D.A., Vale, L.R., Missert, N., and Rosenthal, P.A., **The Critical Current and Normal Resistance of High-T_c Step-Edge SNS Junctions**, IEEE Transactions on Applied Superconductivity, Vol. 5, No. 2, pp. 3405-3409 (June 1995).

We have fabricated high-T_c superconductor-normal-superconductor Josephson junctions with a variety of controlled geometries and measured the resulting dependences of critical current and normal resistance. These studies show that we can adjust our junction parameters over orders of magnitude, thus allowing us to tailor the junctions for a variety of applications.
[Contact: Carl D. Reintsema, (303) 497-5052]

Sauvageau, J.E., Booi, P.A.A., Cromar, M.W., Benz, S.P., Burroughs, C.J., and Koch, J.A., **Superconducting Integrated Circuit Fabrication Process Utilizing Low-Temperature ECR-Based PECVD SiO_2 Dielectric Films**, IEEE Transactions on Applied Superconductivity, Vol. 5, No. 2, pp. 2303-2309 (June 1995).

A superconducting integrated circuit fabrication process has been developed to encompass a wide range of applications such as Josephson voltage standards, VLSI scale array oscillators, SQUIDs, and kinetic-inductance-based devices. An optimal Josephson junction process requires low-temperature processing for all deposition and etching steps. This low-temperature process involves an electron-cyclotron-resonance-based plasma-enhanced chemical vapor deposition (PECVD) of SiO_2 films for interlayer dielectrics. Experimental design and statistical process control techniques have been used to ensure high-quality oxide films. Oxide and niobium etch processes include endpoint detection and controlled overetch of all films. An overview of the fabrication process is presented.
[Contact: Joseph E. Sauvageau, (303) 497-3770]

Antenna Metrology

Released for Publication

Francis, M.H., **A Comparison of K-Correction and Taylor-Series Correction for Probe-Position Errors in Planar Near-Field Scanning**, to be published in the Proceedings of the 17th Annual Meeting and Symposium, Antenna Measurement Techniques Association, Williamsburg, Virginia, November 13-17, 1995.

Two principal error-correction methods have been developed for probe-position errors in planar near-field scanning. The first is the k-correction method, which was largely developed at the Georgia Institute of Technology. The second is the Taylor-series correction, which was developed by Muth and Lewis at the National Institute of Standards and Technology. We investigated these two methods to determine how well the corrected results compare to the uncorrupted far field. For this investigation, we measured a 1.2 m dish at 4 GHz and a 1.2 m by 0.9 phased array at 2.2 GHz. Measurements were made first without position errors and then with deliberate z-position errors. We performed probe-position error correction using both methods and compared the results to the error-free far field. We found that for errors up to $\lambda/4$, the Taylor-series correction fifth-order implementation was slightly better than the k-correction. For errors of $\lambda/2$, the k-correction was better than the Taylor-series.
[Contact: Michael H. Francis, (303) 497-5873]

Guerrieri, J., Canales, N., MacReynolds, K., and Tamura, D., **Element Excitation Analysis on a 60 GHz Phased Array**, to be published in the Proceedings of the 17th Annual Meeting and Symposium, Antenna Measurement Techniques Association, Williamsburg, Virginia, November 13-17, 1995.

The Antenna and Materials Metrology Group of the National Institute of Standards and Technology recently performed a preliminary evaluation of an experimental 60 GHz active array antenna developed for the military services. The antenna was designed using monolithic microwave integrated circuit (MMIC) devices and has an aperture size of 1.0 cm × 1.5 cm with 30 elements.

NIST wanted to determined if the aperture amplitude and phase of an active antenna of this size could be evaluated using planar near-field (PNF) measurement techniques and the Inverse Fast Fourier Transform (FFT). The antenna had lossy

phase shifters that could vary the element excitation by 5 dB.
[Contact: Jeff Guerrieri, (303) 497-3863]

Muth, L.A., **General Order N Analytic Correction of Probe-Position Errors in Planar Near-Field Measurements**, to be published in the Proceedings of the 17th Annual Meeting and Symposium, Antenna Measurement Techniques Association, Williamsburg, Virginia, November 13-17, 1995.

An analytic technique recently developed at NIST to correct for probe position errors in planar near-field measurements has been implemented to arbitrary accuracy. The nth-order correction scheme is composed of an mth-order ordered expansion and a n-m higher-order approximation. Both n and m are arbitrary, and the convergence has been demonstrated for periodic probe position errors as large as 0.9 λ. The technique successfully removes very large probe position errors in the near-field, so that the residual near-field probe position errors are substantially below levels that can be measured on a near-field range. Only the error-contaminated near-field measurements and an accurate probe position error function are needed to be able to implement the correction technique. The method also requires the ability to obtain derivatives of the error-contaminated near field defined on an error-free regular grid with respect to the coordinates. In planar geometry the derivatives are obtained using FFTs, giving an approximate operation count of $3 \cdot 2^{m-1}$ -1 + (n-m) N log N, where N is the number of data points. Efficient computer codes have been developed to demonstrate the technique using computer simulations. The results of simulations are compared to the well-known k correction, which can remove position errors in some direction in k space adequately, but further contaminates the sidelobe levels. The technique presented here corrects for the position errors in all of k space, that is, both in the main beam and all the sidelobes, better than the k correction for a large enough m and n.
[Contact: Lorant A. Muth, (303) 497-3603]

Muth, L.A., Lewis, R.L., and Wittmann, R.C., **Polarimetric Calibration of Reciprocal-Antenna Radars**, to be published in the Proceedings of the 17th Annual Meeting and Symposium, Antenna Measurement Techniques Association, Williamsburg, Virginia, November 13-17, 1995.

We discuss how RCS target depolarization enhances cross-polarization contamination, and we present a graphical study of measurement error due to depolarization by an inclined dihedral reflector.
[Contact: Lorant A. Muth, (303) 497-3603]

Antenna Metrology

Recently Published

Lewis, R.L., **Spherical-Wave Source-Scattering Matrix Analysis of Antennas and Antenna-Antenna Interactions**, NIST Technical Note 1373 (July 1995).

Expressions are presented for describing incoming and outgoing fields about an antenna in terms of a series of exciting and emergent vector spherical-wave functions. The exciting and emergent fields around the antenna's exterior are related to the field in the antenna feed through a source-scattering matrix representation. Series of spherical-wave source-scattering matrix coefficients are used to express more conventional antenna parameters such as gain and receiving cross section. An overview of rotation and translation theorems for transforming vector spherical-wave functions between two distinct coordinate systems is given, followed by a general solution to the problem of expressing the coupling between two coupled antennas in terms of each antenna's spherical-wave source-scattering matrix representation. We go on to consider special results to substantiate our formulation, such as showing equivalence between the coupling equations for transmission in opposite directions when the antennas are reciprocal, showing uniform convergence of some series representations for antenna coupling and simultaneously obtaining a coordinate-system translation theorem for the dyadic Green's function, and showing that our two-antenna coupling equations reduce to expressions for the incident and emergent fields about a single antenna when the other antenna is an elementary dipole. Efficient probe-corrected spherical and hemispherical scanning algorithms are then developed for processing measured near-field data to obtain an antenna's far-field pattern. Finally, we describe a number of self-consistency tests and theoretical-data simulations

that were developed to validate our spherical-scanning algorithm, and we describe an independent experimental verification.
[Contact: Richard L. Lewis, (303) 497-5196]

Noise Metrology

Recently Published

Wait, D.F., **Radiometer Equation for Noise Comparison Radiometers**, IEEE Transactions on Instrumentation and Measurement, Vol. 44, No. 2, pp. 336-339 (April 1995).

A complete radiometer equation is derived and used to develop better corrections and uncertainty estimates. We believe it to be the first thorough analysis of radiometers with unisolated front ends. We show that a corrected unisolated radiometer can have an accuracy similar to that of a well-isolated radiometer. The radiometer error is insignificant for radiometers with 40 dB isolation. However, for high-temperature applications (such as sources and standards above 3000 K), isolation is usually unnecessary.
[Contact: David F. Wait, (303) 497-3610]

Microwave and Millimeter-Wave Metrology

Released for Publication

Jargon, J.A., **A 30 MHz Comparison Receiver**, to be published in the Proceedings of the 1995 Asia-Pacific Microwave Conference, Taejon, Korea, October 10-13, 1995.

The National Institute of Standards and Technology has developed a highly sensitive 30 MHz comparison receiver for detecting low-level radio frequency signals in the nanovolt region. The purpose of this instrument is to detect a null between two signals that can be adjusted in phase and magnitude. This paper contains a description of the receiver, specifications, and theory of operation.
[Contact: Jeffrey A. Jargon, (303) 497-3596]

Jargon, J.A., Marks, R.B., and Williams, D.F., **Coaxial Line-Reflect-Match Calibration**, to be published in the Proceedings of the 1995 Asia-Pacific Microwave Conference, Taejon, Korea, October 10-13, 1995.

We describe a coaxial line-reflect-match calibration that corrects for imperfections in the load used as a match standard. The method provides a practical means of obtaining accurate, wideband calibrations with compact coaxial standard sets. When our load model is valid, the load may be characterized using an additional line of moderate length.
[Contact: Jeffrey A. Jargon, (303) 497-3596]

Marks, R.B., DeGroot, D.C., and Jargon, J.A., **High-Speed Interconnection Characterization Using Time Domain Network Analysis**.

Time domain network analysis (TDNA), formerly a strictly academic exercise, has become a realistic competitor to conventional automatic network analyzers. Off-line processing of data from fast digital sampling oscilloscopes can provide measurements of network parameters with an accuracy that is acceptable for many packaging and interconnect problems at frequencies from dc to over 10 GHz. Since many packaging laboratories have ready access to the required instruments, TDNA brings many advanced measurement capabilities into the hand of engineers to whom a conventional network analyzer is unavailable.
[Contact: Roger B. Marks, (303-497-3037]

Marks, R.B., Jargon, J.A., Pao, C.K., and Wen, C.P., **Electrical Measurements of Microwave Flip-Chip Interconnections**, to be published in the Proceedings of the 1995 International Symposium on Microelectronics, Los Angeles, California, October 24-26, 1995.

We apply custom calibration standards and software to the accurate on-wafer measurement of components on flip-chip co-planar waveguide monolithic microwave integrated circuits. We characterize transmission lines, metal insulator metal capacitors, and spiral inductors and develop equivalent-circuit models. The results are applicable to the development of an accurate computer-aided designed database.
[Contact: Roger B. Marks, (303) 497-3037]

Williams, D.F., **Thermal Noise in Lossy Waveguides**.

This work rigorously treats thermal electromagnetic noise in lossy waveguides and develops explicit modal equivalent-circuit representations for the noise generated by arbitrary passive networks embedded in them. The results show that the formulations in common use are limited to lossless transmission media.
[Contact: Dylan F. Williams, (301) 497-3138]

Williams, D.F., and Schappacher, J.B., **Line-Reflect-Match Calibrations with Nonideal Microstrip Standards**, to be published in the Proceedings of the Automatic Radio Frequency Techniques Group, Scottsdale, Arizona, November 30—December 1, 1995.

We apply a previously developed Line-Reflect-Match calibration that compensates for the nonideal electrical behavior of the match standard to microstrip transmission lines and investigate impedance definitions, standard parasitics, and calibration accuracy.
[Contact: Dylan F. Williams, (303) 497-3138]

Microwave and Millimeter-Wave Metrology

Recently Published

Clague, F.R., **A Calibration Service for Coaxial Reference Standards for Microwave Power**, NIST Technical Note 1374 (May 1995).

A calibration service at the National Institute of Standards and Technology for coaxial microwave power reference standards is described. The service provides measurements of the reference standard effective efficiency from 50 MHz to 18 GHz at a power level of 10 mW. In the Report of Calibration, the effective efficiency is reported in percent. The NIST microwave power standards consists of both a microcalorimeter and an associated reference standard. The reference standard is a bolometric-type power detector (a thermistor mount). The only thermistor mounts accepted for measurement are those constructed to NIST specifications which are compatible with the coaxial microcalorimeter. These thermistor mounts and the automated microcalorimeter are described. A detailed error analysis with an estimate of the calibration uncertainties and their sources is included. The calibration uncertainty, which is quoted as a function of frequency, ranges from about 0.2% at 50 MHz to 0.4% at 18 GHz.
[Contact: Fred R. Clague, (303) 497-5778]

DeGroot, D.C., Beall, J.A., Marks, R.B., and Rudman, D.A., **Microwave Properties of Voltage-Tunable $YBa_2Cu_3O_{7-\delta}/SrTiO_3$ Coplanar Waveguide Transmission Lines**.

To explore the electrical characteristics of monolithic microwave circuits with integrated high-temperature superconductor and ferroelectric materials, we fabricated a series of coplanar waveguide transmission lines in laser-deposited $YBa_2Cu_3O_{7-\delta}$ and $SrTiO_3$ thin films. We characterized the voltage-tunable two-port microwave response of the transmission lines at cryogenic temperatures using a calibrated network analyzer system. Total phase shifts and phase tuning in these devices increased for increasing ferroelectric film thickness with only moderate increases in transmission loss.
[Contact: Donald C. DeGroot, (303) 497-7212]

Electromagnetic Properties

Recently Published

Galt, D., Price, J.C., Beall, J.A., and Harvey, T.E., **Ferroelectric Thin Film Characterization Using Superconducting Microstrip Resonators**, IEEE Transactions on Applied Superconductivity, Vol. 5, No. 2, pp. 2575-2578 (June 1995).

We describe a novel technique for characterizing the dielectric response of ferroelectric thin films at microwave frequencies. The method involves a microstrip resonator which incorporates a ferroelectric capacitor at its center. To demonstrate this method, we have fabricated a superconducting microstrip resonator from a laser-ablated $YBa_2Cu_3O_{7-\delta}$ film on a $LaAlO_3$ (LAO) substrate with a $SrTiO_3$ (STO) capacitor at its center. We report the observed dielectric behavior of the STO laser-ablated film as a function of bias at liquid He and N_2 temperatures and at high and low frequencies. It is observed that the electrically tunable dielectric constant of the STO film is roughly independent of frequency up to 20 GHz (especially at high bias). The loss tangent of the STO/LAO capacitor decreases with increasing bias and is apparently independent of frequency between 6 and 20 GHz.

[Contact: James A. Beall, (303) 497-5989]

Laser Metrology

Recently Published

Leonhardt, R.W., and Scott, T.R., **Deep UV Excimer Laser Measurements at NIST**, Proceedings of SPIE (The International Society for Optical Engineering, P.O. Box 10, Bellingham, Washington 98227-0010), Integrated Circuit Metrology, Inspection, and Process Control IX, Vol. 2439, pp. 448-459 (1995).

The National Institute of Standards and Technology has designed and built two electrically calibrated laser calorimeters as primary standards for absolute energy measurements at the wavelength of 248 nm. Under the sponsorship of SEMATECH, NIST developed the calorimeters to improve measurement of dose-energy in excimer-laser-based microlithography. The calorimeter system can be used to calibrate transfer standards which in turn can be used to calibrate detectors employed for energy measurements of semiconductor wafer exposure. The excimer calorimeter uses a glass filter which functions as a volume absorber that allows collection of nanosecond pulses of laser radiation without suffering damage. The measurement range of the calorimeters is 0.3 to 25 J, but can be extended to 1 mJ with beam splitters. Electrical calibration of the calorimeters shows a standard deviation in the calibration factor of less than 0.5% for entire energy range. The total uncertainty of typical power and energy meter calibrations is approximately 2%.
[Contact: Rodney W. Leonhardt, (303) 497-5162]

Zhang, Z.M., Livigni, D.J., Jones, R.D., and Scott, T.R., **Thermal Modeling and Analysis of Laser Calorimeters**, Proceedings of the 1995 ASME-/AIAA National Heat Transfer Conference, Portland, Oregon, August 6-9, 1995, pp. 1-11.

We performed detailed thermal analysis and modeling of the C-series laser calorimeters at the National Institute of Standards and Technology for calibrating laser power or energy meters. A finite-element method was employed to simulate the space and time dependence of temperature at the calorimeter receiver. The inequivalence in the temperature response caused by different spatial distributions of the heating power was determined. The inequivalence between electrical power applied to front and rear portions of the receiver is $\approx$1.7%, and the inequivalence between the electrical and laser heating is estimated to be <0.05%. The computational results are in good agreement with experiments at the 1% level. The effects of the deposited energy, power duration, and relaxation time on the calibration factor and cooling constant were investigated. This paper provides information for future design improvement on the laser calorimeters.
[Contact: David J. Livigni, (303) 497-5898]

Optical Fiber Metrology

Released for Publication

Schlager, J.B., Mechels, S.E., and Franzen, D.L., **Precise Laser-Based Measurement of Zero-Chromatic-Dispersion Wavelength in Single-Mode Fibers**, to be published in the Conference Digest of the 1996 Conference on Optical Fiber Communications, San Jose, California, February 25—March 1, 1996.

We have developed two laser-based systems for determining the zero-chromatic-dispersion wavelength of multi-kilometer-length optical fibers with a precision of 0.05 nm or better at the 95% confidence level. The first system measures fiber group delay; the second measures differential group delay.
[Contact: John B. Schlager, (303) 497-3542]

Optical Fiber Metrology

Recently Published

Rappaport, A.G., Williams, P.A., Thomas, B.N., Clark, N.A., Ros, M.B., and Walba, D.M., **X-Ray Observation of Electroclinic Layer Constriction and Rearrangement in a Chiral Smectic-A Liquid Crystal**, Applied Physics Letters, Vol. 67, No. 3, pp. 362-364, July 17, 1995.

An X-ray scattering study of electroclinic layer constriction verifies the interpretation of the electroclinic effect as field-induced molecular tilt. The tilt angles deduced from the layer spacing changes are in close agreement with those from

optical measurements. Layer buckling, a consequence of the layer constriction, is also observed and may be the cause of the loss of optical contrast observed in electroclinic devices.
[Contact: Paul A. Williams, (303) 497-3805]

Williams, D.H., Young, M., and Tietz, L.A., **Fiber Coating Diameter: Toward a Glass Artifact Standard**, Proceedings of the 3rd Optical Fibre Measurement Conference, Liège, Belgium, September 25-26, 1995, p. III.2.

This paper proposes a glass fiber, 245 μm in diameter, with an appropriate index of refraction as a standard for the calibration of outer primary coating diameter measurements. Fibers will be manufactured by either a melt process or a draw process. The index of refraction will be measured by the Becke line method and the diameter, with a contact micrometer.
[Contact: Matt Young, (303) 497-3223]

Optical Fiber/Waveguide Sensors

Released for Publication

Day, G.W., **Optoelectronics at NIST**, to be published in the Proceedings of 1995 IEEE Lasers and Electro-Optics Society Annual Meeting, San Francisco, California, October 30—November 2, 1995.

Examples of NIST research in optoelectronics include the development of measurement technology and standards for materials, devices, and manufacturing processes, and the use of optoelectronics in the measurement of other quantities.
[Contact: Gordon W. Day, (303) 497-5204]

Rose, A.H., and Rochford, K.B., **Optical Current Sensor Technologies in Power Utility Applications**, to be published in the Proceedings of EPRI Workshop on Optical Sensors for Utility Transmission and Distribution Applications, Portland, Oregon, July 20-21, 1995.

Optical sensors using optical fiber and thin magneto-optic films are finding increasing use in the transmission and distribution markets of Europe, Japan, and the U.S.A. Both types of sensors electrically isolate measurements from the power potential. However, the two sensor types have cost, stability, and measurement differences that determine the application.
[Contact: Allen H. Rose, (303) 497-5599]

Rose, A.H., and Wyss, J.C., **Self Calibrating Optical Thermometer**, to be published in the Proceedings of SPIE (The International Society for Optical Engineering, P.O. Box 10, Bellingham, Washington 98227-0010), Self-Calibrated Intelligent Optical Sensors and Systems Conference, Philadelphia, Pennsylvania, October 25-26, 1995.

To demonstrate a self-calibrating optical sensor, a computer-controlled optical-thermometer has been built. The self-calibrating thermometer records the temperature with a fiber-optic polarimetric temperature sensor. The wavelength sensitivity of the polarimetric sensor is used to facilitate the recalibration process. The system contains an optical source that can be tuned over approximately a 9 nm wavelength range and a monochromator to measure any shifts in the wavelength of the laser. The monochromator is calibrated with the spectra of a neon discharge lamp.
[Contact: Allen H. Rose, (303) 497-5599]

Williams, P.A., Rose, A.H., Lee, K.S., Conrad, D.C., Day, G.W., and Hale, P.D., **Optical, Thermo-Optic, Electro-Optic, and Photo-Elastic Properties of Bismuth Germanate ($Bi_4Ge_3O_{12}$)**.

To assess the suitability of bismuth germanate as an electro-optic material for high precision applications, we have confirmed and extended previous data on its refractive index, electro-optic tensor element (r_{41}), and thermal expansion coefficient. In addition, we have measured the thermo-optic coefficient (dn/dT), the temperature dependence of the electro-optic effect, and the stress-optic tensor elements. From the stress-optic tensor elements and previously published data, we have computed the strain-optic tensor elements. The refractive index is given, to a good approximation, by the single term Sellmeier equation, $n^2 - 1 = s_o \lambda_o^2/(1 - (\lambda_o/\lambda)^2)$ with $s_o = 95.608\ \mu m^{-2}$ and $\lambda_o = 0.1807\ \mu m$. The thermo-optic coefficient is 3.90×10^{-5} °C and 3.45×10^{-5} °C at wavelengths of 633 nm and 1150 nm, respectively. The electro-optic tensor element varies between about 1.05 and 1.11 pm/V over the spectral range of 550 nm to 1000 nm; its

normalized effective change with temperature is about 1.54 x 10^{-4} °C. The thermal expansion coefficient is 6.3 x 10^{-6} °C over the range from 15 °C to 125 °C. Values for the stress-optic tensor elements are $q_{11} - q_{12} = -2.995 \times 10^{-13}$ m^2/N and $q_{44} = -0.1365 \times 10^{-12}$ m^2/N. The strain-optic tensor elements are $p_{11} - p_{12} = -0.0266$ and $p_{44} = -0.0595$.
[Contact: Paul A. Williams, (303) 497-3805]

Optical Fiber/Waveguide Sensors

Recently Published

Patrick, H., and Gilbert, S.L., **Comparison of UV Photosensitivity and Fluorescence During Fiber Grating Formation**, Proceedings of the Photosensitivity and Quadratic Nonlinearity in Glass Waveguides: Fundamentals and Applications Topical Meeting, Portland, Oregon, September 9-11, 1995, pp. 148-151.

We have conducted a comparison of the UV photosensitivity of optical fiber with the blue fluorescence emitted during the exposure. In a survey of ten non-hydrogen-loaded germanium-doped fibers, we measured the UV photosensitivity and monitored the blue fluorescence during the growth of fiber gratings. Our goal was to determine whether the initial fluorescence, or the change in the fluorescence during exposure, is correlated with the index change. This provides insight into the underlying physical mechanism of UV-induced index change and also determines whether the blue fluorescence can be used as an indicator of the photosensitivity of a fiber.
[Contact: Heather Patrick, (303) 497-6353]

Patrick, H., Gilbert, S.L., Lidgard, A., and Gallagher, M.D., **Annealing of Bragg Gratings in Hydrogen-Loaded Optical Fiber**, Journal of Applied Physics, Vol. 78, No. 5, pp. 2940-2945 (September 1995).

We have conducted a detailed study of the thermal stability of Bragg gratings written in hydrogen-loaded and unloaded germanium-doped optical fiber. Interference of either continuous-wave or pulsed ultraviolet light was used to induce the index modulation gratings. Some gratings were kept at room temperature and others were annealed at fixed temperatures for 10 to 20 h. For temperatures between room temperature and 350 °C, gratings in the hydrogen-loaded fiber showed significantly greater decay than those in the unloaded counterpart. The ultraviolet-induced index modulation in hydrogen-loaded fiber was reduced by 40% after 10 h at 176 °C, whereas it was reduced by only 5% in unloaded fiber under the same conditions. The annealing behavior of gratings written using the pulsed source was identical to that of gratings written with the continuous-wave source, and the thermal stability of gratings in hydrogen-loaded fiber did not depend on the magnitude of the index modulation. We also observed that the annealing of ultraviolet-induced OH absorption in the hydrogen-loaded fiber was not correlated with the grating decay. Our annealing results show that the species responsible for the index change in the hydrogen-loaded fiber are less stable than those in the unloaded fiber.
[Contact: Heather Patrick, (303) 497-6353]

Yang, S., Vayshenker, I., Li, X., Zander, M., and Scott, T.R., **Optical Detector Nonlinearity: Simulation**, NIST Technical Note 1376 (May 1995).

A unified mathematical treatment has been developed for five commonly used measurement methods of optical detector nonlinearity, and a computer simulation was conducted to compare these methods for different measurement conditions and data processing options. The triplet and differential methods are shown to give overall best results, and third- and fourth-order polynomial representations of the measurement result will yield least total error for a common practical measurement system.
[Contact: Igor Vayshenker, (303) 497-3394]

Integrated Optics

Released for Publication

Day, G.W., **Optoelectronics at NIST**, to be published in the Proceedings of 1995 IEEE Lasers and Electro-Optics Society Annual Meeting, San Francisco, California, October 30—November 2, 1995.

[See Optical Fiber/Waveguide Sensors.]

Integrated Optics

Recently Published

Graettinger, T.M., Morris, P.A., Roshko, A., Kingon, A.I., Auciello, O., Lichtenwalner, D.J., and Chow, A.F., **Growth of Epitaxial $KNbO_3$ Thin Films**, Proceedings of the Materials Research Society Symposium, Vol. 341, pp. 265-276 (1994).

$KNbO_3$ possesses high-nonlinear optical coefficients making it a promising material for frequency conversion of infrared light into the visible wavelength range using integrated optical devices. While epitaxial thin films of $KNbO_3$ have previously been grown using ion beam sputtering, defects (i.e., grain boundaries, domains, surface roughness) in these films resulted in high-optical losses and no measurable in-plane birefringence. Previous films were grown on MgO substrates, which have a >4% lattice mismatch with $KNbO_3$. In the work reported here, we have grown films on MGO, $MgAl_2O_4$, and $NdGaO_3$ to investigate the role of lattice mismatch on the resulting film quality. Films have also been grown with and without oxygen ion assistance. The orientations, morphologies, and defects in the films were examined using X-ray diffraction and atomic force microscopy to determine their relationships to the growth conditions and substrate lattice mismatch.
[Contact: Alexana Roshko, (303) 497-5420]

Schaafsma, D.T., and Christensen, D.H., **Cross-Sectional Photoluminescence and Its Application to Buried-Layer Semiconductor Structures**, Journal of Applied Physics, Vol. 78, No. 2, pp. 694-699 (July 15, 1995).

[See Analysis and Characterization Techniques.]

Veasey, D.L., Malone, K.J., Aust, J.A., and Sanford, N.A., **Distributed Feedback Lasers in Rare-Earth-Doped Phosphate Glass**, Proceedings of the 7th European Conference on Integrated Optics, Delft, The Netherlands, April 3-6, 1995, pp. 579-581.

We have successfully demonstrated waveguide lasers operating at 1056.1, 1058.2, and 1062.6 nm in Nd-doped phosphate glass. The waveguides were fabricated by potassium ion exchange from a nitrate melt. Distributed feedback grating patterns were holographically written at 458 nm in photoresist spun on the sample surfaces. The gratings were developed, coated with chromium at a 60-degree evaporation angle, and were then transferred into the glass by argon ion sputtering. Typical laser threshold was 32 mW of absorbed pump power at 805 nm with a corresponding slope efficiency of 2%.
[Contact: David L. Veasey, (303) 497-5952]

Weisshaar, A., Gallawa, R.L., and Goyal, I.C., **Vector and Quasi-Vector Solutions for Optical Waveguide Modes Using Efficient Galerkin's Method with Hermite-Gauss Basis Functions**, Journal of Lightwave Technology, Vol. 13, No. 6, pp. 1795-1800 (August 1995).

An efficient vector formulation and a corresponding quasi-vector formulation for the analysis of optical waveguides are presented. The proposed method is applicable to a large class of optical waveguides with general refractive index profile in a finite region of arbitrary shape and surrounded by a homogeneous cladding. The vector formulation is based on Galerkin's procedure using Hermite-Gauss basis functions. It is shown that use of Hermite-Gauss basis functions leads to a significant increase in computational efficiency over trigonometric basis functions. The quasi-vector solution is obtained from the standard scalar formulation by including a polarization correction. The accuracy of the scalar, vector, and quasi-vector solutions is demonstrated by comparison with the exact solution for the fundamental mode in a circular fiber. Comparison of the modal solutions obtained with the various methods for optical waveguides with square, rectangular, circular, and elliptical core demonstrate the accuracy and advantage of the quasi-vector solution.
[Contact: Robert L. Gallawa, (303) 497-3761]

Other Signal Topics

Recently Published

Wieman, C., Flowers, G., and Gilbert S., **Inexpensive Laser Cooling and Trapping Experiment for Undergraduate Laboratories**, American Journal of Physics, Vol. 63, No. 4, pp. 317-330 (April 1995).

We present detailed instructions for the construction

and operation of an inexpensive apparatus for laser cooling and trapping of rubidium atoms. This apparatus allows one to use the light from low-power diode lasers to produce a magneto-optical trap in a low-pressure vapor cell. We present a design which has reduced the cost to less than $3000 and does not require any machining or glassblowing skills in the construction. It has the additional virtues that the alignment of the trapping laser beams is very easy, and the rubidium pressure is conveniently and rapidly controlled. These features make the trap simple and reliable to operate, and the trapped atoms can be easily seen and studied. With a few milliwatts of laser power, we are able to trap 4 x 10^7 atoms for 3.5 s in this apparatus. A step-by-step procedure is given for construction of the cell, setup of the optical system, and operation of the trap. A list of parts with prices and vendors is given in the Appendix.
[Contact: Sarah Gilbert, (303) 497-3120]

ELECTRICAL SYSTEMS

Power Systems Metrology

Released for Publication

Christophorou, L.G., and Van Brunt, R.J., **Gaseous Dielectrics Research: Possible SF_6 Substitutes**, to be published in the Proceedings of the United States Environmental Protection Agency's Conference on Electrical Transmission and Distribution Systems, Sulfur Hexafluoride, and Atomospheric Effects of Greenhouse Gas Emissions, Washington, D.C., August 9-10, 1995.

Sulfur hexafluoride (SF_6) is the most common insulating gas in enclosed electrical systems to date. It is, however, a potent greenhouse gas and thus, its use could impart fears of environmental costs, regulations, and restrictions, in spite of its current low levels in the environment. An aspect of this potential problem, namely the search for alternative high-voltage insulants, such as high-pressure gaseous dielectrics (e.g., N_2 and N_2/SF_6 mixtures), is addressed in this paper.
[Contact: Loucas G. Christophorou, (301) 975-2432]

Christophorou, L.G., and Van Brunt, R.J., **SF_6 Insulation: Possible Greenhouse Problems and Solutions**, to be published as NISTIR 5685.

Sulfur hexafluoride (SF_6) is the most common insulating gas used in enclosed electrical systems to date. It has been identified, however, as a potent greenhouse gas and thus, its use could impact environmental costs, regulations, and restrictions, in spite of its current low levels in the environment. This potential problem and current efforts in the search for short-term and long-term solutions are briefly outlined and discussed in this report. Limiting the release of SF_6 in the environment, recycling SF_6, and limiting its use, are among the elements of an emerging consensus effort for the short run. A long-term solution may include the search for alternative high-voltage insulants, such as high-pressure gaseous dielectrics (e.g., N_2 and N_2/SF_6 mixtures), and would require accurate measurements and reference data to quantify their physical, chemical, and dielectric properties.
[Contact: Loucas G. Christophorou, (301) 975-2432]

Christophorou, L.G., and Van Brunt, R.J., **SF_6/N_2 Mixtures: Basic and High-Voltage-Insulation Properties**.

The widespread use of SF_6 by the electric power and other industries has led to increased concentrations of SF_6 in the atmosphere. This causes concern as to possible effects on global warming because SF_6 is a potent greenhouse gas. This paper first touches on this issue and then documents the behavior of high-pressure gases such as N_2 and SF_6/N_2 mixtures that can be realistically considered as acceptable intermediate or long-term replacements for pure SF_6 in some high-voltage applications. The possible use of dilute SF_6/N_2 mixtures as an alternative to pure SF_6 for some of industry's insulation needs (albeit at higher pressure) is documented, and existing knowledge on these mixtures and on the individual components (N_2 and SF_6), both basic and applied, is compiled. A guide to existing literature is provided.
[Contact: Loucas G. Christophorou, (301) 975-2432]

Rose, A.H., and Rochford, K.B., **Optical Current Sensor Technologies in Power Utility Applications**, to be published in the Proceedings of EPRI Workshop on Optical Sensors for Utility

Transmission and Distribution Applications, Portland, Oregon, July 20-21, 1995.

[See Optical Fiber/Waveguide Sensors.]

Stricklett, K.L., and Altafim, R.A.C., **Electrohydrodynamic Instability and Electrical Discharge Initiation in Hexane**, to be published in the Proceedings of the Conference on Electrical Insulation and Dielectric Phenomena, Virginia Beach, Virginia, October 22-25, 1995.

An experimental technique is described that tests the hydrodynamic stability of the fluid boundary in a fluid-insulated system: A quasi-uniform field configuration is used, and a pulsed, Nd:YAG laser is employed to create a micro-bubble at the surface of one electrode. The gap is pulse-charged, and the laser is synchronized with the time-of-application of the voltage pulse. Under appropriate experimental conditions of voltage and laser pulse energy, the bubble evolves to produce full electrical breakdown by the onset and propagation of instabilities in the bubble surface. Experimental data obtained in hexane are presented.
[Contact: Kenneth L. Stricklett, (301) 975-3955]

von Glahn, P.G., **Comments on the Digital Processing of Partial Discharge Signals**.

This paper is a discussion by Peter Osvath. Osvath's paper describes some design issues for digital partial discharge instrumentation. This discussion highlights potential problems with Osvath's approach and presents some thoughts on future directions for partial discharge instrumentation design.
[Contact: Peter G. von Glahn, (301) 975-2427]

Power Systems Metrology

Recently Published

Martzloff, F.D., Mansoor, A., Phipps, K.O., and Grady, W.M., **Surging the Upside-Down House: Measurements and Modeling Results**, Proceedings of the Third International Conference on Power Quality End-Use Applications and Perspectives, Amsterdam, The Netherlands, October 24-27, 1994, Part 1, pp. A-1.05, 1-6. [Also, to be published in the Proceedings of the 1995 PQA Conference, New York, New York, May 8-11, 1995.]

Electronic equipment with two input ports, power and communications, can be exposed to damaging differences of voltage between the two ports during surge events. To demonstrate real-world scenarios, a replica of the wiring system in a typical residence was installed in the laboratory. This paper reports selected results from many measurements, and presents the corresponding numerical modeling, thereby leading to mutual validation of the two processes. Two exposure scenarios for producing differences of voltages between the power and data ports of appliances are illustrated. Additional measurements and parametric variations are reported here to characterize the impedance of the various components of the wiring system and the source impedance of the resulting overvoltages appearing between the ports.
[Contact: François D. Martzloff, (301) 975-2409]

Magnetic Materials and Measurements

Released for Publication

Hopkins, P.F., Moreland, J.M., Malhotra, S.S., and Liou, S.H., **Superparamagnetic Magnetic Force Microscopy Tips**.

We report on magnetic force microscopy (MFM) images of a thin-film magnetic recording head taken using batch micromachined silicon tips coated with nanocomposite $Fe_{60}(SiO_2)_{40}$ and $Fe_{70}(SiO_2)_{30}$ films. The small Fe grain size (<10nm) and dilute Fe volume fraction (0.29 to 0.4) of these granular films produce tips of low coercivity, lowered by the superparamagnetic properties of these films. MFM images of current biased heads show reduced tip memory effects compared to images taken with commercially available $Co_{85}Cr_{15}$ coated tips. The gap field is clearly delineated from the pole pieces in the MFM images, providing a means of studying the writing fields with high spatial and magnetic field resolution. Comparison of MFM tip response versus current-bias of the head is also shown.
[Contact: John M. Moreland, (303) 497-3641]

Oti, J.O., Cross, R.W., Russek, S.E., and Kim, Y.K., **Simulating Device Size Effects on Magnetization Pinning Mechanisms in Spin Valves**.

The effects of magnetostatic interactions on the giant magnetoresistive (GMR) response of NiFe/Cu/NiFe spin valves are studied using an analytical model. The model is applicable to devices sufficiently small in size for the magnetic layers to exhibit single-domain behavior. Devices having lengths in the track-width direction of 10 μm and interlayer separations of 4.5 nm are studied. Stripe heights are varied from 0.5 μm to 2 μm, and the thickness of the magnetic layers are varied from 2.5 nm to 20 nm. The magnetization of one magnetic layer is pinned by a transverse pinning field that is varied from zero to 24 kA/m (300 Oe). GMR curves for transverse fields are calculated. At zero external field, the magnetization of the layers shows a tendency to align itself antiparallel in the transverse direction. This results in an offset from the ideal of the biasing of the device. Broadening of the curves due to shape anisotropy occurs with decreasing stripe height and increasing magnetic layer thicknesses, and the magnetization in the pinned layer becomes less stable.
[Contact: John O. Oti, (303) 497-5557]

Oti, J.O., and Kim, Y.K., **Modeling Effects of Temperature Annealing on GMR Response in Discontinuous Multilayer NiFe/Ag Films**.

The giant magnetoresistive (GMR) behaviors of discontinuous double-layer giant magnetoresistive films with different microstructure arising from different annealing conditions are calculated using a numerical micromagnetic model. The considered evolutions of the microstructure are magnetic grain growths in perpendicular and lateral directions in the magnetic layers, and the formation and growth of grain clusters. The GMR response of the films is analyzed in terms of magnetostatic interactions between the magnetic layers and the microstructural geometric effects on the transport properties of the samples.
[Contact: John Oti, (303) 497-5557]

Superconductors

Released for Publication

Cooley, L.D., **Effect of Proximity Length on Flux Pinning in APC Composites: An Overview of APC**.

This paper argues that the lack of adequate high-field pinning in artificial pinning center (APC) composites is an inherent property of a dominant *magnetic* pinning mechanism and the long proximity length of Nb pins. Recent work on APC composites has uncovered trends in the flux-pinning and microstructural data, which hold despite the variety of their designs. By comparing these trends to those of conventional Nb-Ti composites, evidence for magnetic pinning being the dominant flux-pinning mechanism is found. This model departs from the widely accepted view that core-pinning is the dominant pinning mechanism. The parameter that controls the optimization of flux-pinning in the microstructure is the proximity length ϵ_N instead of the diameter of the fluxon core. The optimum bulk pinning force occurs for the best balance of a strong elementary pinning force f_p and a high number density of pins. However, since f_p is maximum when the pin thickness $t \approx \epsilon_N$, the number density of pins can be made to be on the order of the fluxon number density by using artificial pins which have very short proximity lengths. Such pins are most desirable to achieve high J_c at high fields.
[Contact: Lance D. Cooley, (303) 497-7747]

Cooley, L.D., Jablonski, P.D., Heussner, R.W., and Larbalestier, D.C., **Nb-Ti Composite Wires with Artificial Ferromagnetic Pins**.

Flux-pinning data for a Nb_{47}Ti/Fe and a Nb_{55}Ti/Ni composite indicate that ferromagnets pin by a barrier mechanism similar to the mechanism studied by Clem for superconductor/insulator multilayers. However, in contrast to Clem's model, the optimum pin separation d_c for ferromagnetic pins should be ~200 nm, because at smaller pin separations the condition $|\psi|^2 = 0$ at the superconductor/-ferromagnet interface leads to a reduction of T_c and H_{c2}. Nonetheless, we find no indication in the experimental data that pin separations slightly below d_c adversely affect J_c, T_c, or H_{c2}.
[Contact: Lance D. Cooley, (303) 497-7747]

Ekin, J.W., **Electromechanical Properties of Bi-22112 Superconductors**, to be published in the Proceedings of the 9th U.S.-Japan Workshop on High-Field Materials, Wires, and Conductors and Standards Procedures for High-Field Superconducting Wire Testing, Kyoto, Japan (1995).

The axial strain degradation of the critical current of $Bi_2Sr_2Ca_1Cu_2O_8$+x (Bi-2212) round-wire superconductors has been measured for Ag- and AgNiMg-sheathed wires. A direct comparison between Ag- and AgNiMg-sheathed Bi-2212 conductors having the same number of filaments, matrix superconductor ratio, and overall wire diameter shows that the irreversible strain limit for the AgNiMg-sheathed conductors is significantly higher than for the Ag-sheathed conductors. The higher-yield strength of AgNiMg compared with Ag may explain both the increased strain tolerance and lower degradation rate in the AgNiMg-sheathed wires. We observe that, for both types of sheathing materials, Bi-2212 round-wire conductors with filament diameters down to about 0.1 mm have the highest J_c values and the lowest strain limit for irreversible J_c damage.
[Contact: John W. Ekin, (303) 497-5448]

Gregory, E., Gulko, E., Pyon, T., and Goodrich, L.F., **Properties of Internal-Tin Nb_3Sn Strand for the International Thermonuclear Experimental Reactor**.

We report on the design and properties of a Nb_3Sn wire strand developed for the International Thermonuclear Experimental Reactor (ITER). The internal-tin process was employed using 19 subelements, 6 spacers, and a T_a-containing barrier to separate the superconducting core from the Cu stabilizer. Specific values of the four properties -- critical current density J_c, hysteresis losses, residual resistivity ratio RRR, and piece length -- required by the ITER specification are difficult to achieve simultaneously in one strand design. This is particularly true when the strand is Cr plated to prevent sintering and to provide interstrand resistance. Some aspects of conductor design and heat treatment, and how these affect the various properties, including "n" value, are outlined.
[Contact: Loren F. Goodrich, (303) 497-3143]

Yuan, C.W., Zheng, Z., deLozanne, A.L., Tortonese, M., Rudman, D.A., and Eckstein, J.N., **Vortex Images in Thin Films of $YBa_2Cu_3O_{7-x}$ and $Bi_2Sr_2Ca_1Cu_2O_{8+x}$ Obtained by Low Temperature Magnetic Force Microscopy**.

We have imaged vortices in superconducting thin films with a low temperature magnetic force microscope which utilizes microfabricated piezoresistive cantilevers with built-in tips. The films of $YBa_2Cu_3O_{7-x}$ and $Bi_2Sr_2Ca_1Cu_2O_{8+x}$ are made by laser ablation and molecular beam epitaxy, respectively. The vortices usually appear as round features in the non-contact image with a diameter of about one μm or slightly less. In some cases, the position of the vortices is correlated to defects observed in the topographic image of the same area. The vortices move sometimes, especially after taking a topographic (contact mode) scan.
[Contact: David A. Rudman, (303) 497-5081]

<u>Superconductors</u>

Recently Published

Bray, S.L., Ekin, J.W., Waltman, D.J., and Superczynski, M.J., **Quench Energy and Fatigue Degradation Properties of Cu- and Al/Cu-Stabilized NbTi Epoxy-Impregnated Superconductor Coils**, IEEE Transactions on Applied Superconductivity, Vol. 5 - Part I, No. 2, pp. 222-225 (June 1995).

In comparative measurements of small-scale epoxy-impregnated Cu-stabilized and Al-Cu-stabilized NbTi test coils at 4 K and 5 T, the heat energy required to quench the Al-Cu-stabilized coil was 4 to 12 times greater than for the Cu-stabilized coil, depending on the relative operating current. Also, the coil's stabilizer resistivity (ρ) was measured as a function of mechanical fatigue to test for strain-induced degradation. The ρ of the Cu-stabilized coil is relatively unaffected by fatigue, while that of the Al-stabilized coil increases with fatigue. However, in these coils, having a typical stabilizer:superconductor ratio of 4:1, the degradation of the Al-Cu-stabilized coil begins to saturate after several hundred fatigue cycles, and, after 2000 fatigue cycles to 0.2% strain, the ρ of the Al-Cu-stabilized coil is still 2.6 times lower than the ρ of the Cu-stabilized coil. Furthermore, after annealing the Al-Cu-stabilized coil at room temperature for 48 h, the ρ degradation was reduced by 76%. Thus, the use of Al-Cu-stabilizer may offer substantial improvements in magnet stability even where the magnet is subjected to fatigue degradation from repeatedly energizing the magnet.
[Contact: Steven L. Bray, (303) 497-5631]

Ekin, J.W., Russek, S.E., Clickner, C.C., and

Sanders, S.C., **Oxygen Annealing of Ex-Situ YBCO/Ag Thin-Film Interfaces**, IEEE Transactions on Applied Superconductivity, Vol. 5 - Part III, No. 2, pp. 2400-2403 (June 1995).

The resistivity of YBCO/Ag interfaces has been measured for different oxygen annealing temperatures for a series of ex-situ fabricated thin-film contacts having sizes ranging from 16 μm x 16 μm down to 4 μm x 4 μm. The interface resistivity began to decrease after annealing at 300 °C for 10 min. in one atmosphere oxygen. After annealing at 400 °C, the contact resistivity decreased by several orders of magnitude to the 10^{-7} Ω-cm^2 range. The 500-nm thick Ag layer showed massive surface diffusion and agglomeration for annealing temperatures above 400 °C; this temperature, thus represents a practical limit for oxygen annealing the YBCO/Ag interface system for more than 10 min. Rapid cooling of the chip after annealing led to a severe loss of critical current density in the YBCO layer, which could be restored by reannealing and cooling at a slower rate of 50° C/min. The relative shape of the conductance-vs.-voltage characteristics of the YBCO/Ag interface were essentially unaltered by oxygen annealing; the overall parabolic shape, superconducting gap features, and magnetic-scattering zero bias anomaly remained constant, even though the contact conductance increased by several orders of magnitude. These data suggest that the main reduction in the interface resistivity arises from an enhancement of the effective contact area, not from a change in interface conduction mechanism.
[Contact: John W. Ekin, (303) 497-5448]

Goodrich, L.F., Wiejaczka, J.A., and Srivastava, A.N., **Anomalous Switching Phenomenon in Critical-Current Measurements When Using Conductive Mandrels**, IEEE Transactions on Applied Superconductivity, Vol. 5, No. 3, pp. 3442-3444 (September 1995).

NIST and other laboratories have observed an anomalous switching phenomenon that can occur in critical-current measurements of coiled Nb-Ti and Nb_3Sn superconductors when mounted on an electrically-conductive measurement mandrel. During acquisition of the voltage-current (V-I) characteristic, large voltage discontinuities are observed. This switching phenomenon results in a multi-valued V-I curve, and apparently multiple "critical-current" values. An explanation of this phenomenon, some necessary conditions for the switching to occur, as well as methods of detecting the phenomenon, are given.
[Contact: Loren F. Goodrich, (303) 497-3143]

Goodrich, L.F., Wiejaczka, J.A., Srivastava, A.N., Stauffer, T.C., and Medina, L.T., **USA Interlaboratory Comparison of Superconductor Simulator Critical Current Measurements**, IEEE Transactions on Applied Superconductivity, Vol. 5, No. 2, pp. 548-551 (June 1995).

An interlaboratory comparison of critical current (I_c) measurements was conducted on the superconductor simulator, which is an electronic circuit that emulates the extremely nonlinear voltage-current characteristic of a superconductor. These simulators are high-precision instruments, and are useful for establishing the integrity of part of a superconductor measurement system. This study includes measurements from participating U.S. laboratories, with NIST as the central, organizing laboratory. This effort was designed to determine the sources of uncertainty in I_c measurements due to uncertainties in the measurement apparatus, technique, or the analysis system. The participating laboratories measured the superconductor simulator with a variety of methods including dc and pulse. This comparison indicated the presence of systematic biases and higher variability at low voltages in the I_c determinations of the measurement systems. All critical current measurements at a criterion of 10 μV on the I_c simulator were within 2% of the NIST value to nominal critical currents of 2 and 50 A. These results could significantly benefit superconductor measurement applications that require high-precision quality assurance.
[Contact: Loren F. Goodrich, (303) 497-3143]

Goodrich, L.F., Wiejaczka, J.A., Srivastava, A.N., Stauffer, T.C., and Medina, L.T., **First VAMAS USA Interlaboratory Comparison of High Temperature Superconductor Critical Current Measurements**, IEEE Transactions on Applied Superconductivity, Vol. 5, No. 2, pp. 552-555 (June 1995).

We conducted an interlaboratory comparison of critical current (I_c) measurements on $Bi_2Sr_2Ca_2$-

Cu_3O_{10} tapes (2223). This study includes measurements from six participating U.S. laboratories, with NIST as the central, organizing laboratory. A number of specimens were prepared with different degrees of instrumentation to isolate sources of variability. Most of the specimens were pre-measured by NIST to reduce uncertainties due to sample variability. Different specimen routing patterns among the laboratories were implemented to isolate sources of variability due to the specimen's measurement history. This study is similar to other Versailles Project on Advanced Materials and Standards (VAMAS) intercomparisons being performed in Japan and Europe and is the first internationally cooperative interlaboratory comparison of HTS (High Temperature Superconductors) I_c measurements. These are the first steps towards developing standard measurement procedures for HTS.
[Contact: Loren F. Goodrich, (303) 497-3143]

McIntyre, P.C., Cima, M.J., and Roshko, A., **The Effects of Substrate Surface Steps on the Microstructure of Epitaxial $Ba_2YCu_3O_{7-x}$ Thin Films on (001) $LaAlO_3$**, Journal of Crystal Growth, Vol. 149, pp. 64-73 (1995).

The effects of steps in the (001) surface of $LaAlO_3$ substrates on the microstructural evolution of heteroepitaxial $Ba_2YCu_3O_{7-x}$ (BYC) thin films were characterized by high-resolution transmission electron microscopy and atomic force microscopy. Native substrate surface steps acted as nucleation sites for both the *c*-axis normal and *c*-axis in-plane (*a*-axis normal) orientations in BYC films prepared by post-deposition annealing of a precursor film. The density of *c*-axis in-plane BYC grains varied dramatically across the surface of the substrates. In several samples, the spatial pattern of *c*-axis in-plane regions present in the BYC films was similar to the twin structure present in the $LaAlO_3$ substrates. Surface grooves present near twin boundaries in the substrates and lattice rotation of the $LaAlO_3$ during its rhombohedral-cubic phase transition at ~450 °C may produce the large surface steps that act as preferred sites for BYC nucleation.
[Contact: Alexana Roshko, (303) 497-5420]

Roshko, A., Russek, S.E., Trott, K.A., Sanders, S.C., Johansson, M.E., Martens, J.S., and Zhang, D., **Effects of Etching on the Morphology and Surface Resistance of $YBa_2Cu_3O_{7-\delta}$ Films**, IEEE Transactions on Applied Superconductivity, Vol. 5 - Part II, No. 2, pp. 1733-1736 (June 1995).

The changes in surface morphology and surface resistance of sputtered and laser ablated $YBa_2Cu_3O_{7-\delta}$ films both before and after etching have been examined. Six different etchants were used: citric acid, nitric acid, Br-methanol, EDTA, disodium EDTA, and ion milling. The surface morphologies of the films were examined by reflection high-energy electron diffraction and atomic force microscopy, both before and after etching. The surface resistance (R_s) was measured at 94 GHz using a confocal resonator. An amorphous layer was found on the film surfaces after exposure to air. A few of the etches restored some of the surface crystallinity, but most caused increases in the overall surface roughness. Several of the wet etches attacked dislocations. Ion milling caused the largest degradation of surface crystallinity and a corresponding increase in R_s. Some of the chemical etches increased R_s by less than 15%.
[Contact: Alexana Roshko, (303) 497-5420]

Sanders, S.C., Russek, S.E., Clickner, C.C., and Ekin, J.W., **Evidence for Tunneling and Magnetic Scattering at In Situ YBCO/Noble-Metal Interfaces**, IEEE Transactions on Applied Superconductivity, Vol. 5 - Part III, No. 2, pp. 2404-2407 (June 1995).

We report low-temperature conductance data for in-situ $YBa_2Cu_3O_{7-\delta}$ (YBCO)/Ag, YBCO/Au, and YBCO/Pt planar c-axis interfaces. Analysis of the conductance data for these interfaces, which have resistivities as low as $1 \times 10^{-8}\ \Omega\ cm^2$, indicates that tunneling is the predominant transport mechanism. Zero-bias conductance peaks are present for all of the in-situ interfaces. These peaks are analyzed in the framework of the Appelbaum model and are attributed to the presence of isolated magnetic spins at the interface. The presence and similarity of the peaks for each noble-metal overlayer supports the hypothesis that the magnetic spins are inherent to the YBCO surface.
[Contact: Steven C. Sanders, (303) 497-5096]

Sanders, S.C., Sok, J., Finnemore, D.K., and Li, Q., **Thermally Activated Hopping of a Single**

Abrikosov Vortex, Physical Review B, Vol. 47, No. 14, pp. 8996-9000 (1 April 1993-II).

Thermally activated hopping of a single Abrikosov vortex has been investigated for a thin Pb film that was decorated with an artificial pinning structure. To determine the location of the vortex, the Pb film is fabricated to be one electrode of a cross-strip superconductor/normal-metal/insulator/-superconductor Josephson junction. Distortions in the Fraunhofer pattern specify the vortex location. As the temperature is raised toward T_c, the vortex depins from the artificial pinning site and reproducibly moves through the same sequence of other pinning sites before it leaves the junction area of the Pb film. The first thermal depinning occurs when the order parameter of the bulk superconductor is about 20% of the $T = 0$ value. The trajectory is not random.
[Contact: Steven C. Sanders, (303) 497-5096]

Voccio, J.P., Rodenbush, A.J., Joshi, C.H., Ekin, J.W., and Bray, S.L., **The Effect of Magnetic Field Orientation on the Critical Current of HTS Conductor and Coils**, IEEE Transactions on Applied Superconductivity, Vol. 5 - Part II, No. 2, pp. 1822-1825 (June 1995).

The critical current of short samples of high-critical-temperature superconductor multifilamentary conductor and ring-shaped coils has been measured at helium temperatures with varying magnetic field orientation with respect to the conductor. The samples and coil conductor consist of a multifilamentary composite of BSCCO-2223 filaments in a silver matrix. Short conductor samples were tested in a variable temperature system with up to 8 T background field using a sample rotational system. Ring-shaped coils made from the sample type of conductor were exposed to a large background field at liquid helium temperatures and critical current was measured with the ring located at various axial positions within the bore. As the ring moves closer to the end of the magnet, the measured critical current decreases, even though the magnitude of the field to which the ring is exposed decreases. This decrease in J_c is due to the strong anisotropy of the superconductor and is consistent with short sample measurements.
[Contact: John W. Ekin, (303) 497-5448]

Other Electrical Systems Topics

Recently Published

Christophorou, L.G., **Electron Attachment to Excited Molecules**, Proceedings of the International Symposium on Electron- and Photon-Molecule Collisions and Swarms, Berkeley, California, July 22-25, 1995, pp. E-1.

The interactions of slow electrons with molecules, especially the processes of electron attachment, depend rather strongly on the internal energy content of the molecules themselves. As a rule, excited molecules interact with slow electrons with substantially larger cross sections than do ground-state molecules. Studies of electron attachment to vibrationally/rotationally excited, "hot," molecules and especially to electronically excited molecules are rather recent, in contrast to the extensive studies on electron attachment to ground-state molecules which cover many decades. Recent studies on electron attachment to thermally excited (or infrared-laser-excited vibrationally/rotationally excited) molecules showed that the effect of internal energy of a molecule on its electron attachment properties depends on the mode, dissociative or nondissociative, of electron attachment; and recent studies of electron attachment to electronically excited molecules, especially photoenhanced dissociative electron attachment to short- and long-lived excited electronic states of molecules produced directly or indirectly by laser irradiation, are discussed.
[Contact: Loucas G. Christophorou, (301) 975-2432]

ELECTROMAGNETIC INTERFERENCE

Conducted EMI

Recently Published

Martzloff, F.D., Mansoor, A., Phipps, K.O., and Grady, W.M., **Surging the Upside-Down House: Measurements and Modeling Results**, Proceedings of the Third International Conference on Power Quality End-Use Applications and Perspectives, Amsterdam, The Netherlands, October 24-27, 1994, Part 1, pp. A-1.05, 1-6. [Also, to be published in the Proceedings of the 1995 PQA

Conference, New York, New York, May 8-11, 1995.]

[See Power Systems Metrology.]

Radiated EMI

Released for Publication

De Lyser, R.R., Holloway, C.L., Johnk, R.T., Ondrejka, A.R., and Kanda, M., **A New Measure of Quality Factor for Low-Frequency Anechoic Chambers Based on Absorber Reflection Coefficients**.

In this paper, a new chamber quality factor which is based on the decay time of the chamber is introduced. This decay time, in turn, is based on the average power absorbed by the chamber walls. The resulting model is simple and does not require intensive numerical computation. Calculations for the chamber quality factor for anechoic chambers which contain different types of absorbing materials are shown, and an intercomparison of calculated and measured values of decay time for the NIST anechoic chamber are provided.
[Contact: Robert T. Johnk, (303) 497-3737]

Hill, D.A., Camell, D.G., Cavcey, K.H., and Koepke, G.H., **Radiated Emissions and Immunity of Microstrip Transmission Lines: Theory and Measurements**.

We analyze radiation from a microstrip transmission line and calculate total radiated power by numerical integration. Reverberation chamber methods for measuring radiated emissions and immunity are reviewed and applied to three microstrip configurations. Measurements from 200 to 2000 MHz are compared with theory, and excellent agreement is obtained for two configurations that minimize feed cable and finite ground plane effects. Emissions measurements are found to be more accurate than immunity measurements because the impedance mismatch of the receiving antenna cancels when the ratio of the microstrip and reference radiated power measurements is taken. The use of two different receiving antenna locations for emissions measurements illustrates good field uniformity within the chamber.
[Contact: David A. Hill, (303) 497-3472]

Tofani, S., Ossola, P., d'Amore, G., Anglesio, L., Kanda, M., and Novotny, D.R., **Three-Loop Antenna System for Performing Near-Field Measurement of Electric and Magnetic Fields from Video Display Terminals (VDTs)**.

This paper discusses the use of a three-loop antenna system (TLAS) for near-field measurement of electric and magnetic fields from video display terminals (VDTs). We have calculated the electric and magnetic dipole moments to derive the electric and magnetic field patterns in the near-field region. Electric and magnetic fields, emitted by several different models of VDTs, have been evaluated by use of the TLAS and compared with those measured by conventional electric and magnetic-field probes at different distances and directions from VDTs. A good correlation (±1.6 dB) between the two measurement techniques was found. This agreement is within the accuracy (±2 dB) of the conventional field-probe measurements.
[Contact: Motohisa Kanda, (303) 497-5320]

ADDITIONAL INFORMATION

Announcements

Characterization Workshop Proceedings Published

The Proceedings of the International Workshop on Semiconductor Characterization: Present Status and Future Needs is now available through AIP Press. The book *Semiconductor Characterization* covers the unique characterization requirements of both silicon IC development and manufacturing and compound semiconductor materials, devices, and the National Technology Roadmap for Semiconductors. Additional sections discuss technology trends and future requirements for compound semiconductor applications. Recent developments in characterization, including in-situ, in-FAB, and off-line analysis methods are also highlighted. The book provides useful insights on the capabilities of different characterization techniques, gives perspectives on industrial metrology requirements, and explores critical needs and issues in semiconductor metrology research. This book will serve as a base-line reference in this rapidly growing field for the next decade.

Dr. David G. Seiler Appointed Chief of NIST's Semiconductor Electronics Division

On September 1, 1995, David G. Seiler assumed the responsibilities of Chief of the Semiconductor Electronics Division, Electronics and Electrical Engineering Laboratory, at the National Institute of Standards and Technology. Dr. Seiler has been with the Division as leader of the Materials Technology Group since 1988, with an assignment as a NIST Program Office analyst for the past year. Prior to coming to NIST, Seiler was a Regents Professor of Physics at the University of North Texas, had served as a solid state physics program officer in the Division of Materials Research at the National Science Foundation (1985-86), and spent a year's sabbatical at the M.I.T. Francis Bitter National Magnet Laboratory (1980-81). Seiler has made significant contributions to the characterization of various semiconductors and has published over 100 papers on their electrical, optical, and nonlinear optical properties. He also has organized a number of international conferences and workshops on semiconductors and has been the editor of several semiconductor books.

The Semiconductor Electronics Division provides measurement-related infrastructure needed by the semiconductor industry in the areas of semiconductor materials, processing, and integrated circuits. Seiler wants the division to continue to make a significant impact on the semiconductor industry with respect to silicon, through achieving goals outlined in the 1994 Semiconductor Industry Association National Technology Roadmap for Semiconductors. With respect to compound semiconductors, he wants to help industry develop an assessment of the measurement infrastructure required for advances in compound semiconductors, and then help to respond to this assessment.

In the foreword, **Craig Barrett**, Chief Operating Officer at Intel, and **Arati Prabhakar**, Director of NIST, stated that "characterization and modeling of semiconductors are increasingly becoming a crucial part of semiconductor manufacturing. This book provides a concise and effective portrayal of industry characterization needs and the problems that must be addressed by industry, government, and academia to continue the dramatic progress in semiconductor technology."

The work is based on papers given at the International Workshop, held the week of January 30, 1995 at NIST in Gaithersburg, Maryland. Sponsors were: The Advanced Research Projects Agency, SEMATECH, the National Institute of Standards and Technology, The Army Research Office, the U.S. Department of Energy, the National Science Foundation, Semiconductor Equipment and Materials International (SEMI), the Manufacturing Science and Technology Division of the American Vacuum Society, and the Working Group on Electronic Materials of the Committee on Civilian Industrial Technologies.

For additional information, or to order the Proceedings, call the American Institute of Physics toll free at 1-800-809-2247.

List of Publications

Bradford, A.G., **Metrology for Electromagnetic Technology: A Bibliography of NIST Publications**, NISTIR 5040 (September 1995).

This bibliography lists the publications of the personnel of the Electromagnetic Technology Division of NIST during the period from January 1970 through publication of this report. A few earlier references that are directly related to the present work of the Division are also included. This edition of the bibliography is the first since the Electromagnetic Technology Division split into two Divisions, and it includes publications from the areas of cryoelectronic metrology and superconductor and magnetic measurements. The optical electronic metrology section found in earlier editions is now being produced separately by the new Optoelectronics Division of NIST. That companion bibliography to this publication is NISTIR 4041. [Contact: Ann G. Bradford, (303) 497-3678]

Lyons, R.M., **A Bibliography of the NIST Electromagnetic Fields Division Publi-**

cations, NISTIR 5039 (August 1995).

This bibliography lists the publications by the staff of the National Institute of Standards and Technology's Electromagnetic Fields Division for the period January 1970 through July 1995. It supersedes NISTIR 5028 which listed the publications of the Electromagnetic Fields Division from January 1970 through July 1994. Selected earlier publications from the Division's predecessor organizations are included.
[Contact: Ruth Marie Lyons, (303) 497-3132]

Schmeit, R.A., **Electrical and Electronic Metrology: A Bibliography of NIST Electricity Division's Publications, NIST List of Publication 94** (July 1995).

This bibliography covers publications of the Electricity Division (and predecessor organizational units), Electronics and Electrical Engineering Laboratory, National Institute of Standards and Technology, for the period of January 1968 through December 1994. A brief description of the Division's technical program is given in the introduction.
[Contact: Ruth A. Schmeit, (301) 975-2401]

Smith, A.J., and Derr, L.S., **A Bibliography of Publications of the NIST Optoelectronics Division**, NISTIR 5041 (September 1995).

This bibliography lists publications of the staff of the Optoelectronics Division and its predecessor organizational units from 1970 through the date of this report.
[Contact: Annie J. Smith, (303) 497-5342]

Walters, E.J., **National Semiconductor Metrology Program, 1990-1994, NIST List of Publications 103** (March 1995).

This List of Publications includes all papers relevant to semiconductor technology published by NIST staff, including work of the National Semiconductor Metrology Program, the Semiconductor Electronics Division, and other parts of NIST having independent interests in semiconductor metrology. Bibliographic information is provided for publications from 1990 through 1994. Indices by topic area and by author are provided. Earlier reports of work performed by the Semiconductor Electronics Division (and its predecessor divisions) during the period from 1962 through December 1989 are provided in NIST List of Publications 72.
[Contact: E. Jane Walters, (301) 975-2050]

1996 Calendar of Events

March 5-7, 1996 (Austin, Texas)

Twelfth Annual IEEE Semiconductor Thermal Measurement and Management Symposium (SEMI-THERM) 1996. Co-sponsored by NIST, the Symposium will present papers on current thermal management and measurement work on electronic components and systems.
[Contact: David L. Blackburn, (301) 975-2068]

May 6-7, 1996 (Baveno, Italy)

IEEE Workshop on VLSI and Microsystem Packaging Techniques and Manufacturing.

The Workshop is co-sponsored by NIST and IEEE, in cooperation with the European Communities, ESPRII DGIII-Industry, NETPACK (the Network in Microelectronic System Integration Packaging), and the JESSI Organization. Topics to be addressed are: the design and implementation of first-level electronic packaging and the technologies, materials, and equipment for the manufacture of multichip and single-chip packages for VLSI and the new emerging domain of microsensors and microsystems.
[Contact: George G. Harman, (301) 975-2097]

July 16-18, 1996 (San Francisco, California)

SEMICON/West '96, Moscone Center. The NIST National Semiconductor Metrology Program will continue its government-industry liaison support role by exhibiting at SEMICON/West in 1996. For over 40 years, NIST and its predecessor, the National Bureau of Standards, have provided expertise on semiconductor-related issues to industry, government agencies, and academia. Since SEMICON/-West's inception 26 years ago, NIST personnel have provided the same expertise to the show's attendees. NIST's booth is located in Hall 4, Booth 6547. Please stop by and see us!
[Contact: Alice Settle-Raskin, (301) 975-4400]

October 1-3, 1996 (Boulder, Colorado)

Symposium on Optical Fiber Measurements. This Symposium, held at NIST in Boulder, provides a forum for reporting the results of recent measurement research in the area of lightwave communications, including optical fibers. Aspects of optical fiber metrology will be discussed, including attenuation, dispersion, geometry, reflectometry, and connectors; integrated optic devices; laser diode sources and detectors; and system measurements.
[Contact: Douglas L. Franzen, (303) 497-3346]

EEEL Sponsors

National Institute of Standards and Technology
Executive Office of the President
U.S. Air Force
Hanscom Air Force Base; McCellan Air Force Base; Newark Air Force Base; Patrick Air Force Base; Combined Army/Navy/Air Force (CCG); CCG-Strategic Defense Command; CCG-Systems Command; Wright Patterson
U.S. Army
Fort Belvoir; Redstone Arsenal; Combined Army/Navy/Air Force (CCG)
Department of Defense
Advanced Research Projects Agency; Defense Nuclear Agency; National Security Agency
Department of Energy
Building Energy R&D; Energy Systems Research; Fusion Energy; Basic Energy Sciences
Department of Justice
Law Enforcement Assistance Administration
U.S. Navy
CCG, Seal Beach; Office of Naval Research; Naval Research Laboratory; Commanding Officer-San Diego; Naval Surface Warfare Center; Naval Air Systems Command
National Science Foundation
National Aeronautics and Space Administration
NASA Headquarters
Department of Transportation
National Highway Traffic Safety Administration
MMIC Consortium
Nuclear Regulatory Commission
Department of Health and Human Services
National Institutes of Health
Various Federal Government Agencies

NIST SILICON RESISTIVITY SRMs

The Semiconductor Electronics Division of NIST provides Standard Reference Materials (SRMs) for bulk silicon resistivity through the NIST Standard Reference Materials Program. The existing SRMs (on 50 mm wafers) shown in the table below will be augmented with an improved set (on 100 mm wafers) during CY 96-97. NIST efforts to produce the new SRMs have recently received increased emphasis. The earlier set will continue to be available until the supply is exhausted.

The new SRMs have similar values of nominal resistivity as the earlier set, but offer improved uniformity and substantially reduced uncertainty of certified values due both to material and procedural improvements. While it is expected that these wafers will offer considerable utility in calibrating contactless gauges, certification has been performed solely with four-point probe methods. Technical insights presented by the rigorous certification process will be presented in a NIST Special Publication. Individual data for each wafer will be supplied along with the SRM Certificate.

It is expected that the higher resistivity SRMs (2547, 2546) will be available first during CY 96 and be followed closely by SRM 2545. The low resistivity material (SRMs 2542, 2541) is expected to be available by year end. A limited number of SRM 2543 may also be available by year end, with the remainder in early CY 97. Technical issues associated with SRM 2544 will preclude its availability until CY 97.

<table>
<tr><th colspan="5">NIST SILICON BULK RESISTIVITY STANDARD REFERENCE MATERIALS</th></tr>
<tr><th colspan="5">DATE UPDATED: 23 JANUARY 1996</th></tr>
<tr><th>NOMINAL RESISTIVITY (ohm · cm)</th><th><u>OLD SRMs</u></th><th>AVAILABILITY</th><th><u>NEW SRMs</u> (ohm · cm)</th><th>ANTICIPATED AVAILABILITY</th></tr>
<tr><td>0.01</td><td>1523 (one of set of two wafers)</td><td>limited supply</td><td>2541</td><td>CY 96</td></tr>
<tr><td>0.1</td><td>1521 (one of set of two wafers)</td><td>limited supply</td><td>2542</td><td>CY 96</td></tr>
<tr><td>1</td><td>1523 (one of set of two wafers)</td><td>limited supply</td><td>2543</td><td>CY 96-97</td></tr>
<tr><td>10</td><td>1521 (one of set of two wafers)</td><td>limited supply</td><td>2544</td><td>CY 97</td></tr>
<tr><td>25</td><td>1522</td><td rowspan="3">set of three wafers no longer available</td><td>2545</td><td>CY 96</td></tr>
<tr><td>75</td><td>1522</td><td>2546 (100)</td><td>CY 96</td></tr>
<tr><td>180</td><td>1522</td><td>2547 (200)</td><td>CY 96</td></tr>
</table>

The above table will be updated in future issues to reflect changes in availability. Every effort will be made to provide accurate statements of availability; NIST sells SRMS on an as-available basis. For technical information, contact James R. Ehrstein, (301) 975-2060; for ordering information, call the Standard Reference Materials Program Domestic Sales Office: (301) 975-6776.

☆U.S. GOVERNMENT PRINTING OFFICE: 1996 - 404-525/57901

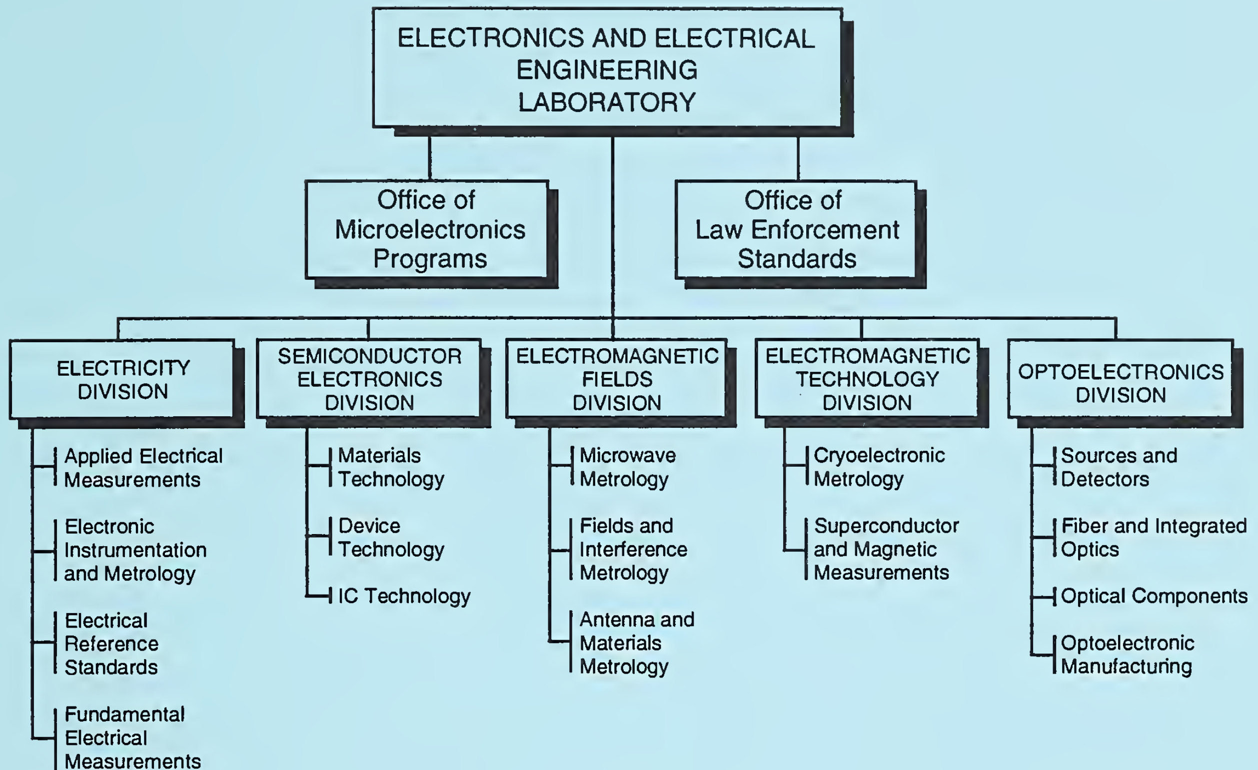

KEY CONTACTS

Laboratory Headquarters (810)	Director, Judson C. French (301) 975-2220
	Deputy Director, Robert E. Hebner (301) 975-2220
	Associate Director, Alan H. Cookson (301) 975-2220
Office of Microelectronics Programs	Director, Robert I. Scace (301) 975-4400
Office of Law Enforcement Standards	Director, Kathleen M. Higgins (301) 975-2757
Electricity Division (811)	Acting Chief, William E. Anderson (301) 975-2400
Semiconductor Electronics Division (812)	Chief, David G. Seiler (301) 975-2054
Electromagnetic Fields Division (813)	Chief, Allen C. Newell (303) 497-3131
Electromagnetic Technology Division (814)	Acting Chief, Richard E. Harris (303) 497-3776
Optoelectronics Division (815)	Chief, Gordon W. Day (303) 497-5204

INFORMATION:

For additional information on the Electronics and Electrical Engineering Laboratory, write or call:

Electronics and Electrical Engineering Laboratory
National Institute of Standards and Technology
Metrology Building, Room B-358
Gaithersburg, MD 20899
Telephone: (301) 975-2220

U.S. DEPARTMENT OF COMMERCE
NATIONAL INSTITUTE OF STANDARDS AND TECHNOLOGY
GAITHERSBURG, MD 20899

OFFICIAL BUSINESS
PENALTY FOR PRIVATE USE, $300

BULK RATE
POSTAGE & FEES PAID
NIST
PERMIT No. G195